Gauge-Aligned Gravity Emergence (GAGE): SM-derived gravitational coupling $G(Q)$

Michael DeMasi, DNP[1]

[1] *Independent Researcher, Milford, CT 06460, USA*

(Dated: November 5, 2025)

Within the SM at $\mu = M_Z$ ($\overline{\text{MS}}$), a unique primitive projector $\boldsymbol{\chi} = (16, 13, 2)$ defines the gauge–log depth $\Xi = \boldsymbol{\chi} \cdot \hat{\boldsymbol{\Psi}}$. An even curvature gate $\Pi(\Xi) = \exp[-(\Delta\Xi)^2/\sigma_\chi^2]$ with $\Pi'(\Xi_{\text{eq}}) = 0$ yields a GR-normalized, massless tensor sector ($m_{\text{PF}} = 0$) and $G(x) = G(M_Z)\Pi(\Xi(x))$, where $G(M_Z) = \hat{\Omega}(M_Z)\hbar c/m_p^2$ and $\hat{\Omega} = \hat{\alpha}_s^{16}\hat{\alpha}_2^{13}\hat{\alpha}^2$ (hats: $\overline{\text{MS}}$ at $\mu = M_Z$). Two direct tests: (i) quadratic lab-null $\Delta G/G \simeq (\Delta\Xi/\sigma_\chi)^2$; (ii) closure/LOO with $\hat{\Omega}(M_Z)/\alpha_G^{(\text{pp})} = 1.09373393$ and $\hat{\alpha}_s^\star(M_Z) = 0.1173411 \pm 1.86 \times 10^{-5}$. Inputs are SM-pinned; metrology is used only *a posteriori*.

Motivation. Despite its precision, the Standard Model has not yielded a self-contained derivation of Newton's constant G_N or a massless spin-2 graviton within its gauge structure. We propose an *alignment principle*: near the electroweak scale, the gauge system aligns with the soft eigenmode of the equilibrium kinetic metric, enforcing parity-even curvature at the lab point. At $\mu = M_Z$ in $\overline{\text{MS}}$, the SNF-certified projector $\boldsymbol{\chi} = (16, 13, 2)$ fixes the gauge–log depth $\Xi = \boldsymbol{\chi} \cdot \hat{\boldsymbol{\Psi}}$; an even gate $\Pi(\Xi)$ with $\Pi'(\Xi_{\text{eq}}) = 0$ yields a GR-normalized, massless spin-2 sector with no new fields or tunable parameters and defines the emergent coupling G. The framework is parameter-free and falsifiable: with $s_\Xi \equiv \Delta\Xi/\sigma_\chi$, $\phi_\chi \equiv \Delta\Xi/\|\boldsymbol{\chi}\|_{\mathbf{K}_{\text{eq}}}$, and $\Lambda_\chi \equiv \sigma_\chi/\|\boldsymbol{\chi}\|_{\mathbf{K}_{\text{eq}}}$, one finds $\Delta G/G = s_\Xi^2 = (\phi_\chi/\Lambda_\chi)^2$; closure is tested *a posteriori* against metrology via $\alpha_G^{(\text{pp})} = G_N m_p^2/(\hbar c)$.

Premise. Work in logarithmic coupling space $\hat{\boldsymbol{\Psi}} = (\ln\hat{\alpha}_s, \ln\hat{\alpha}_2, \ln\hat{\alpha})$, where multiplicative renormalization becomes additive and basis transports are linear [1–3]. We seek a *single*, basis-invariant scalar depth in this space that governs the curvature response and defines the emergent coupling $G(x)$. Its existence is not assumed but must arise from SM structure and be protected by a symmetry enforcing an even equilibrium response (*i.e.*, a null first derivative).

Alignment principle (physical motivation). Let $\mathbf{K}_{\text{eq}} \succ 0$ denote the equilibrium kinetic metric on $\hat{\boldsymbol{\Psi}}$. Small variations organize along its *soft eigenmode*—the direction of minimal kinetic curvature. We find numerically, using SM pins [4, 5], that the gauge system aligns its response along this mode. Alignment has two immediate consequences: (i) **Parity protection.** Near equilibrium, the response is even, so the leading deviation is quadratic in the depth displacement. The resulting *parity-null* is directly testable—any observed linear term falsifies the mechanism. (ii) **Tensor-sector normalization.** With even parity at the laboratory point, the linearized tensor dynamics coincide with GR (luminal helicity-2, no Pauli–Fierz mass). The graviton sector thus *emerges* as the parity-even curvature response of the aligned gauge system [6, 7].

This alignment-first view provides the physical intuition before the algebra: the next sections identify the unique direction (certificate), define the depth Ξ, specify the even gate $\Pi(\Xi)$, derive the β-function for G, and establish closure and falsifiers.

In Fisher-metric terms, alignment corresponds to motion along the soft eigenvector of $\mathbf{K}_{\text{eq}}$—the direction of least informational curvature. Equivalently, systems minimize Fisher resistance by cohering along the soft mode, the information-geometry analog of least action.

Integer certificate and depth. The alignment principle requires a single scalar coordinate in coupling space that remains invariant under renormalization–basis changes. From the one-loop decoupling lattice of the SM, the Smith normal form (SNF) isolates a unique primitive left-kernel generator [8–10],

$$\boldsymbol{\chi} = (16, 13, 2),$$

certifying that only one integer combination of gauge couplings remains invariant under one-loop decoupling transformations (Appelquist–Carazzone regime). This integer projector defines the gauge–log depth

$$\Xi = \boldsymbol{\chi} \cdot \hat{\boldsymbol{\Psi}}, \qquad \hat{\boldsymbol{\Psi}} = (\ln\hat{\alpha}_s, \ln\hat{\alpha}_2, \ln\hat{\alpha}),$$

with local fluctuation $\Delta\Xi = \Xi - \Xi_{\text{eq}}$. Log coordinates render multiplicative renormalization additive and basis transports linear [1, 2]: $\hat{\boldsymbol{\Psi}}' = A\hat{\boldsymbol{\Psi}}$, $\boldsymbol{\chi}' = A^{-\top}\boldsymbol{\chi}$, so $\Xi = \boldsymbol{\chi} \cdot \hat{\boldsymbol{\Psi}}$ is basis-invariant. Under metric transport $K' = A^{-\top}KA^{-1}$,

$$\|\boldsymbol{\chi}\|_K^2 = \boldsymbol{\chi}^\top K\, \boldsymbol{\chi} = \boldsymbol{\chi}'^\top K' \boldsymbol{\chi}',$$

so both $\|\boldsymbol{\chi}\|_K$ and the gate scale $\Lambda_\chi = \sigma_\chi/\|\boldsymbol{\chi}\|_K$ remain invariant under basis choice. The integer certificate, scalar depth, and their transport properties complete the algebraic foundation for the curvature gate introduced next.

SNF certificate (sketch). $\Delta W_{\text{EM}} = \begin{bmatrix} 8 & 8 & 224 \\ 0 & 1 & 18 \end{bmatrix}$ has integer rank 2, giving $\ker_{\mathbb{Z}}(\Delta W_{\text{EM}}) = \text{span}\{\pm\chi_{\text{EM}}\}$ with $\chi_{\text{EM}} = (-10, -18, 1)$ and $\Delta W_{\text{EM}}\chi_{\text{EM}} = 0$. Unimodular transport $M^\top\chi_{\text{EM}} = \boldsymbol{\chi} = (16, 13, 2)$ fixes the primitive generator, unique up to sign (full proof in SM Sec. S1).

Even gate and definition of $G(x)$. Having identified the invariant scalar depth $\Xi = \boldsymbol{\chi}\cdot\hat{\boldsymbol{\Psi}}$, we introduce the curvature-response function (the *gate*) that modulates the emergent gravitational coupling. The gate must satisfy: (i) even parity about equilibrium [$\Pi'(\Xi_{\rm eq}) = 0$]; (ii) analyticity and positivity for all Ξ; (iii) normalization $\Pi(\Xi_{\rm eq}) = 1$ (recovering GR at equilibrium); and (iv) minimal parameter freedom.

A minimal analytic, even, and positive form satisfying these is the Gaussian gate

$$\Pi(\Xi) = \exp\Big[-\frac{(\Delta\Xi)^2}{\sigma_\chi^2}\Big], \qquad \Pi'(\Xi_{\rm eq}) = 0, \quad \Pi(\Xi_{\rm eq}) = 1,$$

which enforces parity-even curvature modulation and smooth suppression beyond the Planck-thin envelope ($|\Delta\Xi| \sim \sigma_\chi$). With $s_\Xi = \Delta\Xi/\sigma_\chi$, $\phi_\chi = \Delta\Xi/\|\boldsymbol{\chi}\|_{\mathbf{K}_{\rm eq}}$, and $\Lambda_\chi = \sigma_\chi/\|\boldsymbol{\chi}\|_{\mathbf{K}_{\rm eq}}$, the laboratory null becomes $\Delta G/G = s_\Xi^2 = (\phi_\chi/\Lambda_\chi)^2$. The width σ_χ is fixed by Fisher curvature from SM covariance at $\mu = M_Z$ [4, 5, 11], leaving no tunable parameters.

Gate parity. If Π is even and C^2 near $\Xi_{\rm eq}$, then $\Pi'(\Xi_{\rm eq}) = 0$ and $\Pi(\Xi_{\rm eq}+\Delta\Xi) = 1-(\Delta\Xi)^2/\sigma_\chi^2+\mathcal{O}((\Delta\Xi)^4)$; any $\mathcal{O}((\Delta\Xi))$ term falsifies parity or alignment. Writing the laboratory template as

$$\frac{\Delta G}{G} = A\,s + B\,s^2 + \mathcal{O}(s^3), \qquad s \equiv \frac{\Delta\Xi}{\sigma_\chi},$$

an even gate predicts $A = 0$, $B = 1$. Equivalently, in the ϕ_χ normalization,

$$\frac{\Delta G}{G} = A'\phi_\chi + B'\phi_\chi^2 + \ldots, \qquad A' = 0, \quad B' = 1/\Lambda_\chi^2.$$

Any reproducible odd term ($A \neq 0$ or $A' \neq 0$) falsifies alignment parity.

Definition (natural units). In natural units ($\hbar = c = 1$), the SM fixes the gravitational coupling via the dimensionless product

$$G \equiv \frac{\Omega}{m_p^2}, \qquad \Omega \equiv \alpha_s^{16}\alpha_2^{13}\alpha^2, \qquad G(x) = G\,\Pi(\Xi(x)). \tag{1}$$

For SI units, restore $\hbar c$:

$$G(M_Z) = \frac{\hat{\Omega}(M_Z)\,\hbar c}{m_p^2}, \qquad \hat{\Omega} = \hat{\alpha}_s^{16}\hat{\alpha}_2^{13}\hat{\alpha}^2. \tag{2}$$

$$\boxed{\Omega \;=\; \hat{\alpha}_s^{16}\,\hat{\alpha}_2^{13}\,\hat{\alpha}^2} \qquad \boxed{G \;=\; \frac{\Omega}{m_p^2}}$$

$$\boxed{\frac{G_*\,\Pi\Big(\hat{\Xi}\Big)}{G_*} \;=\; \Pi\Big(\hat{\Xi}\Big) \;=\; \exp\Big[-\frac{(\hat{\Xi}-\hat{\Xi}^{(\rm eq)})^2}{\sigma_\chi^2}\Big]}$$

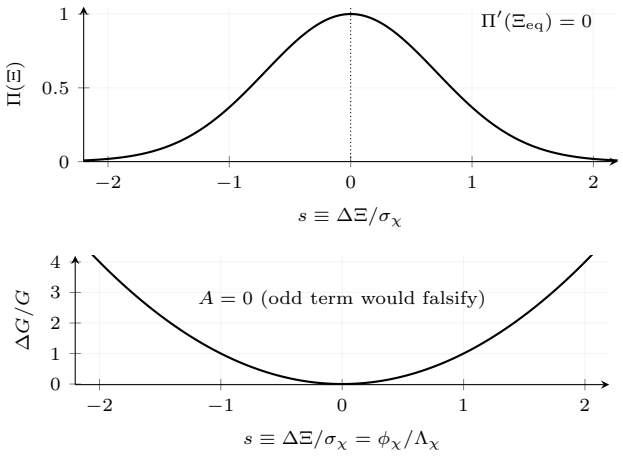

FIG. 1. Even gate $\Pi(\Xi) = \exp[-(\Delta\Xi)^2/\sigma_\chi^2]$ vs $s = \Delta\Xi/\sigma_\chi$ with parity condition $\Pi'(\Xi_{\rm eq}) = 0$, enforcing the quadratic response $\Delta G/G \simeq (\Delta\Xi)^2/\sigma_\chi^2 = \phi_\chi^2/\Lambda_\chi^2$. Any odd term As would falsify alignment.

Parity-even lab null and tensor sector. Even parity of the gate enforces a quadratic curvature response near equilibrium. With $\mathbf{K}_{\rm eq} \succ 0$ and alignment of $\hat{\chi} = \boldsymbol{\chi}/\|\boldsymbol{\chi}\|_{\mathbf{K}_{\rm eq}}$ to the soft eigenvector of $\mathbf{K}_{\rm eq}$,

$$\frac{\Delta G}{G} \simeq \frac{(\Delta\Xi)^2}{\sigma_\chi^2} = \frac{\phi_\chi^2}{\Lambda_\chi^2}, \qquad \phi_\chi = \frac{\boldsymbol{\chi}^\top(\hat{\boldsymbol{\Psi}} - \langle\hat{\boldsymbol{\Psi}}\rangle)}{\|\boldsymbol{\chi}\|_{\mathbf{K}_{\rm eq}}}, \tag{3}$$

$$\Lambda_\chi = \frac{\sigma_\chi}{\|\boldsymbol{\chi}\|_{\mathbf{K}_{\rm eq}}}. \tag{4}$$

This constitutes the *quadratic lab null*: any linear term in $\Delta G/G$ falsifies parity or alignment.

No h–ϕ mixing at linear order. $S \supset \frac{M_{\rm P}^2}{2}\Pi(\Xi)R$. Since $\Pi'(\Xi_{\rm eq}) = 0$, the variation $\delta\Omega = M_{\rm P}^2\Pi'(\Xi_{\rm eq})\,\delta\Xi$ vanishes, removing the $(g_{\mu\nu}\Box - \nabla_\mu\nabla_\nu)\delta\Omega$ term at $\mathcal{O}(h)$. The remaining equation $\mathcal{E}_{\mu\nu}^{\ \alpha\beta}h_{\alpha\beta} = 0$ is the Lichnerowicz operator with $m_{\rm PF} = 0$.

Because $\Pi'(\Xi_{\rm eq}) = 0$, the linearized equation reduces to

$$\Delta_L h_{\mu\nu} \equiv -\Box h_{\mu\nu} = 0, \tag{5}$$

so the tensor mode is GR-normalized, massless, and luminal (helicity-2) [6, 7, 12, 13].

Pinned scales. With $K_{\rm eq} \succ 0$, the gate scale is

$$\Lambda_\chi = \frac{\sigma_\chi}{\|\chi\|_{K_{\rm eq}}}. \tag{6}$$

From SM pins at $\mu = M_Z$ one finds $\sigma_\chi = 247.683$ and $\|\chi\|_{K_{\rm eq}} = 17.6278$, giving $\Lambda_\chi = 14.0507$ (derivation in the Supplement).

TABLE I. Equilibrium kinetic metric $K_{\rm eq}$: eigenvalues and alignment diagnostics.

Eigenvalues $(\lambda_1, \lambda_2, \lambda_3)$	$\|\chi\|_{K_{\rm eq}}$	$\cos\theta_K$	ε_χ
(0.7243, 2.0156, 3.2599)	17.6278	0.9999999998	$< 10^{-8}$

Running of G and Ward-flatness. Because G is composed of SM couplings, its renormalization follows theirs. Differentiating $\Xi = \boldsymbol{\chi}\cdot\hat{\boldsymbol{\Psi}}$ gives

$$\beta_\Xi \equiv \frac{d\Xi}{d\ln Q} = 16\frac{\beta_{\alpha_s}}{\alpha_s} + 13\frac{\beta_{\alpha_2}}{\alpha_2} + 2\frac{\beta_\alpha}{\alpha} = 0$$

(1 loop; Ward-flat).

Thus Ξ and G are stationary at one loop, avoiding basis artifacts [1, 2]. Preregistered flatness windows and masks are evaluated in the SM; Fig. 2 shows the monitor $F(Q)$ within bounds.

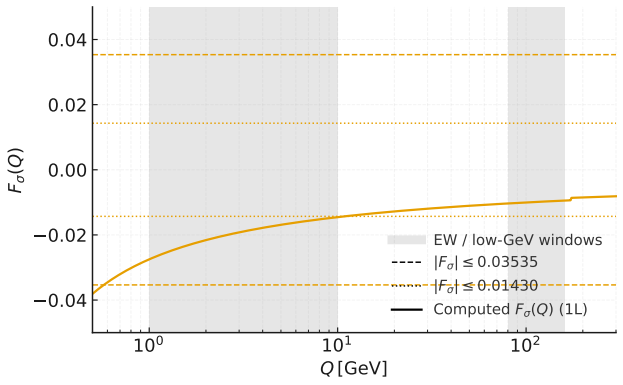

FIG. 2. Projected flatness monitor $F(Q)$ within preregistered electroweak and low-GeV windows. One-loop flatness corresponds to $\beta_\Xi = 0$; mild threshold kinks appear outside the EW window.

Beyond equilibrium, slow variation of $K_{\rm eq}$ produces adiabatic tracking of the soft mode (dynamic alignment) and a small two-loop drift (quantified in the Supplement).

The running of G follows directly:

$$\beta_G \equiv \frac{d\ln G}{d\ln Q} = 16\frac{\beta_{\alpha_s}}{\alpha_s} + 13\frac{\beta_{\alpha_2}}{\alpha_2} + 2\frac{\beta_\alpha}{\alpha} = 0 + O(\hat\alpha_i^2), \quad (7)$$

so G is flat at one loop with bounded higher-order drift [14]. Physically,

$$G(x) = G\,\Pi(\Xi(x)), \qquad G = \frac{\Omega}{m_p^2}. \quad (8)$$

At $\mu = M_Z$ ($\overline{\rm MS}$), comparison is made *a posteriori* to the metrological coupling $\alpha_G^{(\rm pp)}$ [15, 16].

Closure and prediction. The *closure test* links the SM invariant to metrology:

$$\hat\Omega(M_Z) = \hat\alpha_s^{16}\hat\alpha_2^{13}\hat\alpha^2 \stackrel{?}{=} \alpha_G^{(\rm pp)} \equiv \frac{G_N m_p^2}{\hbar c}. \quad (9)$$

If equality holds within uncertainties,

$$G(\Xi_{\rm eq}) = \frac{\hat\Omega(M_Z)\hbar c}{m_p^2} = G(M_Z). \quad (10)$$

Inverting gives the leave-one-out (LOO) forecast,

$$\hat\alpha_s^\star(M_Z) = \left[\frac{\alpha_G^{(\rm pp)}}{\hat\alpha_2^{13}\hat\alpha^2}\right]^{1/16} = 0.1173411 \pm 1.86\times10^{-5}, \quad (11)$$

consistent with the PDG mean (-0.73σ) [4, 5]. The closure ratio

$$\frac{\hat\Omega(M_Z)}{\alpha_G^{(\rm pp)}} = 1.09373393 \quad (+9.37\%) \quad (12)$$

serves as the empirical benchmark [4, 11, 15, 16].

Matching (UV→IR). Define the IR normalization via a dimensionless matching factor Z_G:

$$G(M_Z) = \frac{\hat\Omega(M_Z)\,\hbar c}{m_p^2}, \qquad G_N \equiv Z_G\,G(M_Z), \quad (13)$$

$$Z_G = \frac{\alpha_G^{(\rm pp)}}{\hat\Omega(M_Z)} = 0.91430\ (-8.57\%). \quad (14)$$

This Z_G absorbs scheme, threshold, and higher-order effects; the full budget is detailed in the Supplement.

Helicity scale. At equilibrium, soft-mode alignment fixes

$$\Lambda_\chi = \frac{\sigma_\chi}{\|\chi\|_{K_{\rm eq}}} = 14.0507\ (\approx 14.05), \quad (15)$$

$$\omega_{\rm hel} = \Lambda_\chi^{-1}, \quad (16)$$

$$T_{\rm hel} = 2\pi\,\Lambda_\chi \simeq 88\,t_P. \quad (17)$$

This *Planck-thin curvature envelope* sets the coherence length of the emergent tensor mode and bounds the quadratic response $\Delta G/G \simeq \phi_\chi^2/\Lambda_\chi^2$ (see SM Sec. S8).

Falsifiers (any suffices). The construction is parameter-free; any single failure falsifies it:

1. **Non-unique integer certificate.** SNF must yield a unique primitive left-kernel generator $\boldsymbol{\chi} = (16, 13, 2)$; any alternate integer solution of comparable norm breaks the projection symmetry [8–10].

2. **Odd (linear) curvature response.** With $\Pi'(\Xi_{\rm eq}) = 0$, a measured linear term As in $\Delta G/G = As + Bs^2 + \ldots$ (where $s = \Delta\Xi/\sigma_\chi$) contradicts the quadratic lab-null in Eq. (4). *Example (illustrative):* taking $s = 9$ from SM pins gives $\Delta G/G \simeq s^2 = (\phi_\chi/\Lambda_\chi)^2 = 1.32\times10^{-3}$, accessible to symmetric $\pm s$ clock/torsion tests; fits must be consistent with $A = 0$.

3. **Tensor-sector anomaly.** Any Pauli–Fierz mass or non-luminal dispersion violates GR-normalized propagation (Eq. (5)) [7, 12, 13].

4. **Metric instability or misalignment.** $K_{\rm eq} \succ 0$ with $\cos\theta_K \simeq 1$ must hold; a negative eigenvalue or deviation beyond ε_χ signals ghost/locking failure (Table 1).

5. **Ward-flatness violation.** The projected flow must satisfy $\beta_\Xi = 0$ within preregistered EW and low-GeV masks (Eq. ()); significant drift implies RG-scheme dependence or breakdown of aligned projection [1, 2].

6. **Closure or LOO failure.** Deviation of $\hat{\Omega}/\alpha_G^{(\rm pp)}$ from unity beyond pinned uncertainties (Eq. (12)), or $\hat{\alpha}_s^\star(M_Z)$ outside PDG bounds (Eq. (11)), falsifies identification of G as SM-derived [4, 5, 15, 16].

Implications. Gravity emerges as the parity-even curvature response of the Standard Model gauge sector, with

$$G(x) = G(M_Z)\,\Pi(\Xi(x))$$

fixed entirely by $\{\hat{\alpha}_s, \hat{\alpha}_2, \hat{\alpha}\}$ at $\mu = M_Z$ [4–6, 11]. Two direct signatures make the framework falsifiable: (i) the quadratic lab-null $\Delta G/G \simeq (\Delta\Xi/\sigma_\chi)^2$, and (ii) the closure ratio $\hat{\Omega}/\alpha_G^{(\rm pp)} = 1.09373393$. Any reproducible odd-parity term or closure mismatch beyond pinned uncertainties would refute the mechanism [7, 12, 13].

The spurion-even gate and χ-projection imply a conserved alignment current,

$$J_\chi^\mu = \Pi(\Xi)\,\chi^\top K_{\rm eq}\,\partial^\mu\hat{\Psi},$$
$$\partial_\mu J_\chi^\mu = 0 + \mathcal{O}\big((\Delta\Xi)^3, 2\text{L drift}, \varepsilon_\chi\big), \qquad (18)$$

the Noether current associated with rigid depth shifts of Ξ at equilibrium. This conservation law is the gauge-depth analog of energy–momentum conservation under spacetime translations: alignment preserves curvature "energy" within the gauge sector. Operationally, any reproducible odd (linear) response [$A \neq 0$ in $\Delta G/G = As + Bs^2 + \cdots$] corresponds to $\partial_\mu J_\chi^\mu \neq 0$ and thus falsifies alignment.

Scope note. This Letter derives the gravitational coupling G from SM couplings and demonstrates empirical closure. Dynamic tensor-sector extensions—including the helicity frequency, Planck-thin envelope, drift law, and the conserved alignment current—are detailed in the Supplemental Material. All analytic derivations and pinned numerical checks are reproducible from the accompanying `GAGE_repo`. A companion study will extend the alignment–conservation framework to a fully dynamical formulation, developing the stress-energy, effective Lagrangian, geometric-fiber, informational, and temporal extensions that complete the GAGE description of gravity.

This work was conducted independently with no external funding. The author thanks the Particle Data Group (PDG), CODATA, Overleaf, and Python for open-access tools and data. An AI-assisted writing tool (OpenAI ChatGPT) was used for language editing and organizational assistance; all scientific content and responsibility rest with the author. The author declares no competing interests.

Data availability All data supporting this work (pins, equations, figure data, and scripts) are included in the Letter, the Supplemental Material, and the accompanying `GAGE_repo`; additional materials are available from the author upon reasonable request.

[1] S. Weinberg, *The Quantum Theory of Fields, Vol. 2: Modern Applications* (Cambridge University Press, Cambridge, UK, 1996).
[2] M. E. Peskin and D. V. Schroeder, *An Introduction to Quantum Field Theory* (Addison-Wesley, Reading, MA, 1995).
[3] P. Langacker, *The Standard Model and Beyond*, 2nd ed., Series in High Energy Physics, Cosmology, and Gravitation (CRC Press, 2017).
[4] S. Navas *et al.* (Particle Data Group), Phys. Rev. D **110**, 030001 (2024), and 2025 update.
[5] T. Dorigo and M. Tanabashi, in *Review of Particle Physics*, edited by Particle Data Group (Oxford University Press, 2025) p. 083C01, published in Prog. Theor. Exp. Phys. 2025 (8), 083C01.
[6] S. M. Carroll, *Spacetime and Geometry: An Introduction to General Relativity* (Addison-Wesley, 2004).
[7] C. M. Will, Living Rev. Relativ. **17**, 4 (2014).
[8] T. Appelquist and J. Carazzone, Phys. Rev. D **11**, 2856 (1975).
[9] R. Kannan and A. Bachem, SIAM J. Comput. **8**, 499 (1979).
[10] M. Newman, Linear Algebra Appl. **254**, 367 (1997).
[11] J. Erler *et al.*, in *Review of Particle Physics* (Particle Data Group, 2024).
[12] B. Bertotti, L. Iess, and P. Tortora, Nature **425**, 374 (2003).
[13] R. Abbott *et al.* (LIGO Scientific Collaboration and Virgo Collaboration and KAGRA Collaboration), Phys. Rev. D (2021), combined bound $m_g \leq 1.27 \times 10^{-23}\,\mathrm{eV}/c^2$ (90% C.L.), arXiv:2112.06861 [gr-qc].
[14] F. Jegerlehner, Nucl. Part. Phys. Proc. **303–305**, 1 (2018), see also arXiv:1705.00263.
[15] P. J. Mohr, D. B. Newell, B. N. Taylor, and E. Tiesinga, Rev. Mod. Phys. **97**, 025002 (2025).
[16] D. Robinson and P. A. Zyla, in *Review of Particle Physics* (Particle Data Group, 2024) topical review, revised 2024.

Supplemental Material for: Gauge-Aligned Gravity Emergence (GAGE)

Michael DeMasi DNP

November 5, 2025

S0. Notation, pins, and conventions

Provenance and sources. All numerical inputs, constants, and coupling data used herein are taken from established references. The Standard Model framework and renormalization conventions follow Weinberg [1], Peskin–Schroeder [2], and Langacker [3]. Decoupling and integer-lattice methods follow Appelquist–Carazzone [4], Kannan–Bachem [5], and Newman [6]. Numerical pins and covariance values are drawn from the Particle Data Group and CODATA [7–10]. Gravitational and metrological comparisons reference Carroll [11], Will [12], Bertotti [13], and Abbott *et al.* (LVK) [14]. Running of couplings follows Jegerlehner [15]. All calculations are performed within $\overline{\text{MS}}$ at $\mu = M_Z$, with no external data sources beyond these references.

Purpose. This Supplemental Material provides the derivations, numeric checks, and reproducibility details referenced in the Letter. It fixes all symbols, evaluation points, and unit conventions, and defines the error-propagation and covariance rules used in tables and figures.

Contents. Hatted couplings; $\mu = M_Z$; $\overline{\text{MS}}$ scheme; PDG/CODATA pins with uncertainties; unit policy; error-propagation rules; equilibrium metric K and eigenvalues; Smith–normal–form certificate for $\boldsymbol{\chi}$; Fisher-width derivation of σ_χ; Ward-flatness masks; closure and leave-one-out tests; reproducibility script and checksum manifest.

Coordinates and logs Work in log–coupling space with hats denoting $\overline{\text{MS}}$ at $\mu = M_Z$:

$$\hat{\boldsymbol{\Psi}} = \big(\ln \hat{\alpha}_s,\ \ln \hat{\alpha}_2,\ \ln \hat{\alpha}\big), \qquad \boldsymbol{\chi} = (16, 13, 2), \qquad \hat{\Xi} = \boldsymbol{\chi}\cdot\hat{\boldsymbol{\Psi}}$$

and the SM-internal invariant

$$\hat{\Omega} \equiv e^{\hat{\Xi}} = \hat{\alpha}_s^{16}\, \hat{\alpha}_2^{13}\, \hat{\alpha}^2 \,.$$

All EFT derivations in this SM proceed in log space; metrology targets are used only later (S5) for closure/LOO validation, not as inputs.

Units policy (concise) **SM pins:** $\overline{\text{MS}}$ at $Q = M_Z$ (hats by default) (SM pins @ M_Z, $\overline{\text{MS}}$)
EFT derivations: natural units ($\hbar = c = 1$), with explicit $\hbar c$ only when mapping back to SI
Metrology targets: SI values (PDG/CODATA) used only in S5 for closure/LOO, never upstream

Gate and metric

$$\frac{G\,\Pi\big(\hat{\Xi}\big)}{G} = \Pi\Big(\hat{\Xi}\Big) = \exp\Big[-\frac{(\hat{\Xi} - \hat{\Xi}^{(\text{eq})})^2}{\sigma_\chi^2}\Big], \qquad \mathbf{K}_{\text{eq}} \succ 0, \quad \|\mathbf{v}\|^2_{\mathbf{K}_{\text{eq}}} = \mathbf{v}^\top \mathbf{K}_{\text{eq}} \mathbf{v}$$

with $\hat{\Xi}^{(\text{eq})} = \hat{\Xi}\big|_{\mu=M_Z}$, gate width σ_χ, and gate scale $\Lambda_\chi = \sigma_\chi / \|\boldsymbol{\chi}\|_{\mathbf{K}_{\text{eq}}}$. Even parity ($\partial_\Xi \Pi|_{\hat{\Xi}^{(\text{eq})}} = 0$) enforces the quadratic lab-null

$$\frac{\Delta G}{G} \simeq \frac{\Delta \hat{\Xi}^2}{\sigma_\chi^2} \qquad \text{with} \qquad \Delta\hat{\Xi} = \hat{\Xi} - \hat{\Xi}^{(\text{eq})} \,.$$

Notation Summary. Located at end of the document. Core scheme/pin conventions follow PDG/CODATA; the Ward-flatness projector and the one-loop identity $\beta_\Xi = 0$ (PRL Eq. (14)) are used later in S5.

Alignment tolerance We define ε_χ to capture residual misalignment and modeling tolerances near equilibrium (e.g., $1 - \cos\theta$, gate-slope leakage, numerical conditioning). Unless stated otherwise, we assume a uniform bound $\varepsilon_\chi \leq 10^{-8}$ (see S2.3,S2.7).

Equilibrium convention Pins are $\overline{\text{MS}}$ at $Q = M_Z$; we set $\Pi(\hat{\mathbf{\Psi}}_{\text{eq}}) = 1$ so $G\,\Pi\Big(\hat{\Xi}\Big)\,|_{\text{eq}} = G$. Any identification with metrology (e.g., $G \stackrel{?}{=} G_{\text{N}}$) is tested only in S5.

Pins and sources (SM pins @ $\mu = M_Z$; metrology targets in S5 only) Table 2 lists *inputs used in derivations* (SM pins); Table 3 lists *closure targets not used as inputs* (metrology). See PRL Table I and Secs. "Running of G and Ward-flatness"–"Closure and prediction" for definitions. SM pins and electroweak conventions follow PDG; SI targets follow CODATA.

Error propagation and correlations Unless stated, use linearized Gaussian propagation in vector form:

$$\text{Cov}(f) = J\,\text{Cov}(x)\,J^\top, \qquad J_{ai} = \partial_{x_i} f_a, \qquad \delta f^2 = \nabla f^\top\,\text{Cov}(x)\,\nabla f.$$

For logarithms,

$$\delta(\ln x) \simeq \frac{\delta x}{x}, \qquad \text{Cov}(\ln x, \ln y) \simeq \frac{\text{Cov}(x,y)}{xy}.$$

Inputs and correlations Include PDG/CODATA covariances where provided (e.g., components entering the running of $\hat{\alpha}$ to M_Z). When unavailable, treat inputs as independent and propagate to derived quantities (e.g., $\hat{\alpha}_2 = \hat{\alpha}/\sin^2\hat{\theta}_{\text{W}}$) via the Jacobian above. All reported uncertainties are 1σ.

Log-space propagation Quantities defined in log coordinates (e.g., $\hat{\mathbf{\Psi}}$, $\hat{\Xi}$) use the same rules; returns to linear variables use $\sigma(y) \approx y\,\sigma(\ln y)$.

Metrology (target-only) handling Closure/LOO covariance, metrology depths, and any optional cross-covariances are handled in S5. We do not use metrology in upstream derivations.

Cross-references and reproducibility Definitions of Ω, closure, and LOO appear in PRL Eqs. (7), (18), and (19). The SM mirrors the Letter: S1 (SNF certificate), S2 (alignment principle), S3 (gate and parity lemma), S4 (tensor sector / no PF mass), S5 (Ward-flatness), S6 (closure and LOO), S7 (environmental lab-null), S8 (helicity scales).

Versioning and reproducibility All pins in Tables 2, 3, 4, 5, and 6 are frozen to the cited PDG/CODATA releases and mirrored locally. Section S9 points to the Repo's `pins.json` (SI; $\overline{\text{MS}}$ at $\mu = M_Z$) and build scripts that regenerate the S0 tables and figure data from source pins. The build is deterministic (no network); SHA-256 hashes are emitted for all artifacts, and any drift indicates a pin or version change. Monte Carlo confirmation of closure/LOO appears only in the SM (Sec. S6.8) and reproduces the linearized propagation. The Repo remains deterministic (no RNG) and regenerates numeric tables and figure data from pinned inputs only.

Reproduction (pointer to Repo) S9 summarizes inputs/outputs and checksums; the complete, executable workflow lives in the accompanying Repo document (source of truth). From the Repo:

- `pins.json` and `keq.json` (MS at $\mu = M_Z$); code derives $\hat{\alpha}_2 = \hat{\alpha}/\sin^2\hat{\theta}_W$
- one-command rebuild: `bash build.sh` *(or Windows* `build_win.bat`*)* $\rightarrow$ regenerates numeric tables and figure data from pins
- optional metrics: `src/metric_eigs.py` emits `metric_results.json` (K_{eq} eigs/evecs, $\|\chi\|_K$, Λ_χ, alignment)
- deterministic run; SHA-256 of all artifacts recorded in `SHA256SUMS.txt`

S9 records filenames, versions, and hashes matching the Repo; code listings are omitted here by design.

Vector form (Jacobian rule) For a vector map $y = f(x)$ with inputs $x = (x_1, \ldots, x_n)$ and outputs $y = (y_1, \ldots, y_m)$,

$$\mathrm{Cov}(y) = J\,\mathrm{Cov}(x)\,J^\top, \qquad J_{ij} = \frac{\partial y_i}{\partial x_j}.$$

Log domain

Work with MS couplings at $\mu = M_Z$: $\hat{\alpha}_i \in \{\hat{\alpha}_s, \hat{\alpha}_2, \hat{\alpha}\}$ and define $\xi_i = \ln \hat{\alpha}_i$. The SM invariant

$$\hat{\Omega} = \prod_i \hat{\alpha}_i^{\chi_i} = \hat{\alpha}_s^{16}\hat{\alpha}_2^{13}\hat{\alpha}^2$$

satisfies

$$\ln \hat{\Omega} = \sum_i \chi_i\,\xi_i,$$

with linearized propagation

$$\delta(\ln \hat{\Omega})^2 = \sum_i \chi_i^2\,\delta\xi_i^2 + 2\sum_{i<j}\chi_i\chi_j\,\mathrm{Cov}(\xi_i, \xi_j).$$

For small relative errors,

$$\delta(\ln \hat{\alpha}_i) \simeq \frac{\delta\hat{\alpha}_i}{\hat{\alpha}_i}, \qquad \mathrm{Cov}(\ln \hat{\alpha}_i, \ln \hat{\alpha}_j) \simeq \frac{\mathrm{Cov}(\hat{\alpha}_i, \hat{\alpha}_j)}{\hat{\alpha}_i\hat{\alpha}_j}.$$

Example (derived SU(2) coupling) With $\hat{\alpha}_2 = \hat{\alpha}/\sin^2\hat{\theta}_{\mathrm{W}}$,

$$\ln \hat{\alpha}_2 = \ln \hat{\alpha} \;-\; \ln\big(\sin^2\hat{\theta}_{\mathrm{W}}\big), \quad \sigma^2\big(\ln \hat{\alpha}_2\big) = \sigma^2\big(\ln \hat{\alpha}\big) + \sigma^2\big(\ln(\sin^2\hat{\theta}_{\mathrm{W}})\big) - 2\,\mathrm{Cov}\Big(\ln \hat{\alpha}, \ln(\sin^2\hat{\theta}_{\mathrm{W}})\Big),$$

and $\sigma(\hat{\alpha}_2) \approx \hat{\alpha}_2\,\sigma\big(\ln \hat{\alpha}_2\big)$.

Derived inputs (closed forms used throughout) (i) SU(2) coupling

$$\hat{\alpha}_2 = \hat{\alpha}/\sin^2\hat{\theta}_{\mathrm{W}}.$$

In linear variables (set Cov = 0 unless specified):

$$\delta\hat{\alpha}_2^2 = \Big(\tfrac{1}{\sin^2\hat{\theta}_{\mathrm{W}}}\Big)^2\delta\hat{\alpha}^2 + \Big(\tfrac{\hat{\alpha}}{(\sin^2\hat{\theta}_{\mathrm{W}})^2}\Big)^2\delta\big(\sin^2\hat{\theta}_{\mathrm{W}}\big)^2 - 2\,\frac{\hat{\alpha}}{(\sin^2\hat{\theta}_{\mathrm{W}})^3}\,\mathrm{Cov}\big(\hat{\alpha}, \sin^2\hat{\theta}_{\mathrm{W}}\big).$$

Equivalently, in logs,

$$\delta\big(\ln \hat{\alpha}_2\big)^2 = \delta\big(\ln \hat{\alpha}\big)^2 + \delta\big(\ln(\sin^2\hat{\theta}_{\mathrm{W}})\big)^2 - 2\,\mathrm{Cov}\big(\ln \hat{\alpha}, \ln(\sin^2\hat{\theta}_{\mathrm{W}})\big), \quad \mathrm{Cov}\big(\ln \hat{\alpha}, \ln(\sin^2\hat{\theta}_{\mathrm{W}})\big) \simeq \frac{\mathrm{Cov}\big(\hat{\alpha}, \sin^2\hat{\theta}_{\mathrm{W}}\big)}{\hat{\alpha}\,\sin^2\hat{\theta}_{\mathrm{W}}}.$$

(ii) Projection depth and certificate

$$\hat{\Xi}^{(\mathrm{eq})} = \boldsymbol{\chi}\cdot\big(\ln \hat{\alpha}_s, \ln \hat{\alpha}_2, \ln \hat{\alpha}\big) = 16\,\ln \hat{\alpha}_s + 13\,\ln \hat{\alpha}_2 + 2\,\ln \hat{\alpha}.$$

Work in the independent basis $x = \big(\ln \hat{\alpha},\ \ln(\sin^2\hat{\theta}_{\mathrm{W}}),\ \ln \hat{\alpha}_s\big)$ with $\ln \hat{\alpha}_2 = \ln \hat{\alpha} - \ln(\sin^2\hat{\theta}_{\mathrm{W}})$:

$$\hat{\Xi}^{(\mathrm{eq})} = 15\,\ln \hat{\alpha} - 13\,\ln(\sin^2\hat{\theta}_{\mathrm{W}}) + 16\,\ln \hat{\alpha}_s, \qquad g_\Xi = (15,\,-13,\,16),$$
$$\sigma^2(\hat{\Xi}^{(\mathrm{eq})}) = g_\Xi^\top\,\mathrm{Cov}(x)\,g_\Xi, \qquad \sigma(\Omega) \simeq \Omega\,\sigma(\hat{\Xi}^{(\mathrm{eq})}).$$

Ward-flatness prereg thresholds Define $F(Q) = \mathrm{d}\hat{\Xi}/\mathrm{d}\ln Q$ and the normalized monitor $F_\sigma(Q) = F(Q)/\sigma_\chi$ with masks around thresholds. The preregistered bounds are on F_σ:

$$\text{EW } [80, 160]\text{ GeV}: \ \|F_\sigma\|_\infty \le 0.01430,\ \mathrm{RMS}(F_\sigma) \le 0.01372,\ |\langle F_\sigma\rangle| \le 0.01372,$$
$$\text{Low-GeV } [1, 10]\text{ GeV}: \ \|F_\sigma\|_\infty \le 0.03535,\ \mathrm{RMS}(F_\sigma) \le 0.02622,\ |\langle F_\sigma\rangle| \le 0.02585.$$

Notes: Bounds are preregistered from the max across 1L/off and 2L/off runs with a 1.5× inflation and include masked thresholds.

S1. Smith–Normal–Form (SNF) certificate for $\boldsymbol{\chi} = (16, 13, 2)$

Goal Show that $\boldsymbol{\chi}$ is fixed by integer structure alone (unique primitive generator up to sign), independent of masses, scales, or scheme choices within the admissible class.

Standing assumptions SM with three families and one Higgs doublet; GUT-normalized hypercharge ($\alpha_1 = \frac{5}{3}\alpha_Y$); mass-independent scheme with Appelquist–Carazzone decoupling. Fix a single $U(1)_Y$ integerization so that $U(1)$ weights are integers for each light set:

$$w_1^{(\mathrm{f})} = 12\sum_{\mathrm{Weyl}} Y^2, \qquad w_1^{(\mathrm{s})} = 3\sum_{\mathrm{scalars}} Y^2.$$

For $H \sim (\mathbf{1}, \mathbf{2}, \frac{1}{2})$, $\sum Y^2 = 2\times(\frac{1}{2})^2 = \frac{1}{2} \Rightarrow w_1(H) = 3$. The ordering of $(\hat{\alpha}_s, \hat{\alpha}_2, \hat{\alpha})$ is a notational convention; permutations simply relabel the components of $\boldsymbol{\chi}$ while the kernel direction (and $\Xi = \boldsymbol{\chi}^{\mathsf{T}}\Psi$) is basis-invariant.

S1.1 Construction recipe (per multiplet)

Per–multiplet weights and integerization. For each light multiplet f in an admissible window $\mathcal{W}$,

$$\begin{aligned} &\text{Weyl:} && w_3(f) = 4\,T_{SU(3)}(f)\,d_{\mathrm{spect}}(f), && w_2(f) = 4\,T_{SU(2)}(f)\,d_{\mathrm{spect}}(f), \\ &\text{scalar:} && w_3(f) = 1\cdot T_{SU(3)}(f)\,d_{\mathrm{spect}}(f), && w_2(f) = 1\cdot T_{SU(2)}(f)\,d_{\mathrm{spect}}(f), \end{aligned}$$

and choose a single $U(1)_Y$ integerizer so the hypercharge column is integral:

$$w_1^{(\mathrm{f})} = 12\sum_{\text{Weyl in } f} Y^2, \qquad w_1^{(\mathrm{s})} = 3\sum_{\text{scalars in } f} Y^2.$$

Here $T_{SU(N)}$ is the Dynkin index ($T(\mathbf{3}) = T(\mathbf{2}) = \frac{1}{2}$), and d_{spect} counts spectator multiplicities (e.g., color for $SU(2)$ weights and weak multiplicity for $SU(3)$ weights). GUT normalization is used for hypercharge: $\alpha_1 = \frac{5}{3}\alpha_Y$.

Window vectors and differences. Sum the weights across the light content of the window:

$$b^{(\mathcal{W})} = \begin{pmatrix} \sum_f w_3(f) \\ \sum_f w_2(f) \\ \sum_f w_1(f) \end{pmatrix} \in \mathbb{Z}^3,$$

then form the integer *difference stack* over admissible window pairs $\{(\mathcal{W}_i, \mathcal{W}_j)\}$:

$$\Delta b^{(ij)} = b^{(\mathcal{W}_i)} - b^{(\mathcal{W}_j)}, \qquad \Delta W = \begin{bmatrix} (\Delta b^{(i_1 j_1)})^{\top} \\ (\Delta b^{(i_2 j_2)})^{\top} \\ \vdots \end{bmatrix} \in \mathbb{Z}^{m\times 3}.$$

Adjoint self–contributions cancel in Δb, exposing the rank–2 lattice used for SNF.

Sanity check (electromagnetic basis). After EWSB, use $w_{\mathrm{EM}} = w_2 + \frac{5}{3}w_1 \Rightarrow 3w_{\mathrm{EM}} = 3w_2 + 5w_1 \in \mathbb{Z}$, so the $(SU(3), SU(2), \mathrm{EM})$ basis keeps exact integers for certification.

S1.2 Worked integer kernel (by hand, no SNF)

$$\chi_{\mathrm{EM}} = (-10, -18, 1), \qquad \gcd(10, 18, 1) = 1 \text{ (primitive)}.$$

In the $(SU(3), SU(2), \mathrm{EM})$ basis the two-row difference stack is

$$\Delta W_{\mathrm{EM}} = \begin{bmatrix} 8 & 8 & 224 \\ 0 & 1 & 18 \end{bmatrix} \in \mathbb{Z}^{2\times 3}.$$

Solve $\Delta W_{\rm EM}\,\chi_{\rm EM}=0$ over $\mathbb{Z}$: second row gives $\chi_2=-18\,\chi_3$; first row gives $8\chi_1+8\chi_2+224\chi_3=0\Rightarrow 8\chi_1+8(-18)\chi_3+224\chi_3=0\Rightarrow\chi_1=-10\,\chi_3$. Choosing $\chi_3=1$ yields the *primitive* generator

$$\boxed{\chi_{\rm EM}=(-10,-18,1)\ ,}\qquad \gcd(10,18,1)=1.$$

Transport to the canonical basis Let $A\in\mathrm{GL}(3,\mathbb{Z})$ be the unimodular change-of-columns from the EM stack to the canonical (w_3,w_2,w_1) basis printed below. Kernel covectors transport contravariantly:

$$\boxed{\chi\ =\ A^{-\mathsf{T}}\,\chi_{\rm EM}}\ .$$

Evaluating with the A (denoted M below) gives

$$\boxed{M^{\top}\chi_{\rm EM}=(16,13,2)\equiv\boldsymbol{\chi}}\ .$$

SNF note The Smith invariants of $\Delta W_{\rm EM}$ are $[1,8]$ (rank 2), with a trailing zero column; hence $\ker_{\mathbb{Z}}(\Delta W_{\rm EM})$ is one–dimensional and generated by $\pm\chi_{\rm EM}$.

SNF (explicit). For $\Delta W_{\rm EM}=\begin{bmatrix}1&1&28\\0&1&18\end{bmatrix}$, there exist unimodular $U\in GL(2,\mathbb{Z})$, $V\in GL(3,\mathbb{Z})$ such that

$$U\,\Delta W_{\rm EM}\,V=\mathrm{diag}(1,\,8,\,0)\,,$$

so rank $=2$ and there is a single zero invariant.

S1.3 Window differences and the integer row lattice

For a momentum window $\mathcal{W}$ with light content $\mathcal{S}_{\mathcal{W}}$, define integerized 1L weights

$$b^{(\mathcal{W})}=\begin{pmatrix}\sum w_3\\ \sum w_2\\ \sum w_1\end{pmatrix}\in\mathbb{Z}^3,$$

with Weyl $w_{3,2}=4\,T_{SU(3,2)}\,d_{\rm spect}$ and scalar $w_{3,2}=1\cdot T_{SU(3,2)}\,d_{\rm spect}$, and w_1 as above. For admissible windows $\{\mathcal{W}_i\}$ form differences

$$\Delta b^{(ij)}=b^{(\mathcal{W}_i)}-b^{(\mathcal{W}_j)},\qquad \Delta W=\begin{bmatrix}(\Delta b^{(i_1j_1)})^{\top}\\(\Delta b^{(i_2j_2)})^{\top}\\ \vdots\end{bmatrix}\in\mathbb{Z}^{m\times 3}.$$

Lemma (row–lattice invariance). Any two admissible stacks $\Delta W,\Delta W'$ are related by unimodular row operations (adding/removing differences; reordering) and appending/canceling common adjoint self-terms. Hence their integer row lattices coincide and their left kernels over $\mathbb{Z}$ are identical.

$$M=\begin{bmatrix}-5&-3&-2\\2&1&1\\2&1&0\end{bmatrix},\qquad \det M=-1,\qquad M^{\top}\chi_{\rm EM}=(16,13,2)\,.$$

Proof sketch. Differences generate the same subgroup as absolute rows modulo a common reference. Appending/removing a difference corresponds to adding/removing an integer row; permutations and sign flips are unimodular. Common adjoint self-terms cancel in any row difference. □

S1.4 Two physical differences (explicit tallies)

Using $T(\mathbf{3})=T(\mathbf{2})=\frac{1}{2}$ and spectator multiplicities (weak multiplicity as spectator for $SU(3)$ weights; color multiplicity as spectator for $SU(2)$ weights), the integerized one–loop weights sum as follows.

One SM generation (five Weyl multiplets).

$$SU(3):\quad w_3(Q_L)=4\cdot\tfrac{1}{2}\cdot 2=4,\qquad w_3(u_R)=4\cdot\tfrac{1}{2}\cdot 1=2,\qquad w_3(d_R)=4\cdot\tfrac{1}{2}\cdot 1=2$$
$$\Rightarrow \sum w_3=8,$$
$$SU(2):\quad w_2(Q_L)=4\cdot\tfrac{1}{2}\cdot 3=6,\qquad w_2(L_L)=4\cdot\tfrac{1}{2}\cdot 1=2\ \Rightarrow\ \sum w_2=8,$$
$$U(1)_Y\ \text{(global integerizer)}:\quad w_1=12\sum_{\text{Weyl}} Y^2=12\big[\tfrac{1}{6}+\tfrac{4}{3}+\tfrac{1}{3}+\tfrac{1}{2}+1\big]=40.$$

Hence

$$\Delta b_{\text{gen}}=(8,\,8,\,40).$$

One Higgs doublet (complex scalar). For $Y=+\frac{1}{2}$ and two weak components,

$$w_2(H)=1\cdot\tfrac{1}{2}\cdot 1=1,\qquad w_1(H)=3\sum_{\text{scalars}} Y^2=3\cdot\tfrac{1}{2}=3,\qquad w_3(H)=0,$$

so

$$\Delta b_H=(0,\,1,\,3).$$

(Any overall common integer factor on a *row* does not affect the *primitive* kernel.)

Integer kernel and cross–check. Stacking these differences gives

$$\Delta W=\begin{pmatrix}8 & 8 & 40\\ 0 & 1 & 3\end{pmatrix},\qquad \Delta W\,\chi=0.$$

Solving over $\mathbb{Z}$ yields the unique primitive generator

$$\chi=(16,\,13,\,2),$$

identical to the EM–stack/SNF certificate. Thus the tally route reproduces the same integer kernel, closing the algebraic–physical loop and fixing χ by integer structure alone.

S2. Alignment as a Symmetry-Locking Principle

Statement. Let $\mathbf{K}_{\text{eq}}\succ 0$ be the equilibrium field-space metric and $\boldsymbol{\chi}=(16,13,2)$ the SNF-certified projector. Define $\hat{\chi}=\boldsymbol{\chi}/\left\|\boldsymbol{\chi}\right\|_{\mathbf{K}_{\text{eq}}}$ and let e_{soft} be the normalized soft eigenvector of $\mathbf{K}_{\text{eq}}$. The *alignment condition* is

$$\cos\theta\ =\ \hat{\chi}^{\top}\,\mathbf{K}_{\text{eq}}\,e_{\text{soft}}\ \geq\ 1-\varepsilon_{\chi},$$

with fixed tolerance $\varepsilon_{\chi}\ll 1$ (reported in SM). When alignment holds, the gauge–log depth $\hat{\Xi}=\boldsymbol{\chi}\cdot\hat{\boldsymbol{\Psi}}$ isolates the soft direction and the parity-even gate $\Pi\Big(\hat{\Xi}\Big)$ projects the gauge sector onto a single scalar depth.

Consequences. (i) *Even-parity protection.* A spurion $\mathbb{Z}_2$ symmetry $\hat{\Xi}\to-\hat{\Xi}$ with Π invariant implies

$$\partial_{\Xi}\Pi\Big(\hat{\Xi}\Big)\Big|_{\hat{\Xi}^{(\text{eq})}}=0\quad\Rightarrow\quad\text{no linear response; } m^2_{\text{PF}}=0,$$

to all loop orders near equilibrium. Renormalization can shift $(\sigma_{\chi},\mathbf{K}_{\text{eq}})$ but cannot generate an odd term.
(ii) *Tensor sector.* Around the lab point (Minkowski) the Lichnerowicz operator reduces to

$$\Delta_L h_{\mu\nu}\ =\ -\Box h_{\mu\nu}=0\quad\Rightarrow\quad\omega^2=\mathbf{k}^2,\ \lambda=\pm 2\ \text{(massless, luminal)}.$$

(iii) *Quadratic lab-null.* The near-eq. response is

$$\frac{\Delta G}{G}\ \simeq\ \frac{\Delta\hat{\Xi}^2}{\sigma_{\chi}^2}=\frac{\phi_{\chi}^2}{\Lambda_{\chi}^2},\qquad \phi_{\chi}=\Delta\hat{\Xi}/\left\|\boldsymbol{\chi}\right\|_{\mathbf{K}_{\text{eq}}},\quad \Lambda_{\chi}=\sigma_{\chi}/\left\|\boldsymbol{\chi}\right\|_{\mathbf{K}_{\text{eq}}}.$$

Falsifier from misalignment. If $\cos\theta < 1 - \varepsilon_\chi$, an odd (linear) term is generically induced in a lab fit

$$\frac{\Delta G}{G}(s) = A\,s + B\,s^2 + \dots,$$

violating the parity null ($A = 0$). Significant misalignment therefore falsifies the model.

Motivation (minimal). Alignment is the universal tendency of coupled fields to cohere along the softest kinetic mode of a positive-definite metric K. In GAGE, the certified integer projector $\boldsymbol{\chi}$ aligns with the soft eigenvector of $\mathbf{K}_{\rm eq}$, enforcing even response and a massless, luminal tensor sector. Analogous locking appears in magnetic ordering, superconductivity, and Higgs vacuum alignment (qualitative context; not inputs).

S2.1 Minimal alignment functional. Let unit order parameters $u_i(x) \in \mathbb{R}^d$ with metrics $K_i \succ 0$ and couplings γ_1, γ_2. Define

$$\mathcal{A}[u] = \int d^D x \Big[\tfrac{1}{2} \sum_i (\partial u_i)^\top K_i (\partial u_i) - \frac{1}{N} \sum_{i<j} (\gamma_1\, u_i \cdot u_j + \gamma_2 (u_i \cdot u_j)^2) \Big], \qquad \|u_i\| = 1.$$

Diagnostics $m = \|\langle u \rangle\|$, $C = \frac{1}{N}\sum_i u_i u_i^\top$, and $\rho = \lambda_{\max}(C)/\mathrm{Tr}(C)$ measure coherence ($m \in [0,1]$, $\rho \in [1/d, 1]$). **Lemma.** For $K \succ 0$ and couplings above a threshold γ_c, minimizers align $\langle u \rangle$ with the soft eigenvector $e_{\rm soft}$ of K up to $O(\kappa_{\rm gap}^{-1})$; orthogonal fluctuations are gapped. **Map to GAGE.** $u \,\|\, \hat{\chi}$, $K \to \mathbf{K}_{\rm eq}$, $\Xi = \boldsymbol{\chi} \cdot \hat{\boldsymbol{\Psi}}$, and even $\Pi(\Xi)$ enforces $\frac{\Delta G}{G} \simeq \phi_\chi^2 / \Lambda_\chi^2$.

S2.2 Phase variant ($\mathbf{S}^1$). For phases θ_i,

$$\mathcal{A}_\theta[\theta] = \int d^D x \Big[\tfrac{\kappa}{2} \sum_i |\nabla \theta_i|^2 - \frac{K}{N} \sum_{i<j} \cos(\theta_i - \theta_j) \Big],$$

whose ordered phase satisfies $\partial_\mu \theta_i \approx \partial_\mu \theta_j$, corresponding to alignment of phase gradients.

S2.3 Conservation form (near equilibrium). Define the alignment current

$$J_\chi^\mu = \Pi(\Xi)\; \boldsymbol{\chi}^\top \mathbf{K}_{\rm eq}\, \partial^\mu \hat{\boldsymbol{\Psi}},$$

which reduces after one contraction to $J_\chi^\mu = \Pi(\Xi)\; \partial^\mu \Xi$. Using $\Pi'(\Xi_{\rm eq}) = 0$ and the Ξ equation of motion,

$$\partial_\mu J_\chi^\mu = 0 + O\big((\Delta\Xi)^3,\ \text{2Loop drift},\ \varepsilon_\chi\big), \qquad \varepsilon_\chi \le 10^{-8}.$$

Any measured odd term $A \neq 0$ in $\frac{\Delta G}{G} = A\,s + B\,s^2 + \dots$ gives $\partial_\mu J_\chi^\mu \neq 0$ and falsifies alignment.

S2.4 Information–geometry view The Fisher curvature along depth,

$$\kappa_\chi \equiv \frac{1}{\sigma_\chi^2} = \partial_{\Delta\Xi}^2 [-\ln \Pi(\Xi)]\big|_{\rm eq},$$

defines the local informational metric. Alignment is motion along the soft eigenvector of $K_{\rm eq}$, i.e., the direction of least Fisher curvature (least informational resistance).

S2.5 Falsifiers and caveats Lab template: $\Delta G/G = A\,s + B\,s^2 + \cdots$, $s = \Delta\Xi/\sigma_\chi$. Alignment predicts $A = 0,\ B = 1$. Additional falsifiers: failure of rank-1 coherence ($\rho \not\to 1$), or locking to a non-soft mode at fixed $K_{\rm eq}$. Boundary/disorder can produce modulated or defect states; diagnose via the most unstable Fourier mode of the quadratic expansion. Tolerance: $\varepsilon_\chi \le 10^{-8}$ (see S2.3, S0).

S2.6 Cross-domain statement Across spins, phases, and gauge directions, alignment is symmetry-locking to the soft mode of K, quantified by (m, ρ) with $m = \|\langle u \rangle\|$ and $\rho = \lambda_{\max}(C)/\mathrm{Tr}(C)$. GAGE is the SM realization with $u \,\|\, \hat{\chi}$ and $K \equiv K_{\rm eq}$.

S2.7 Noether-style derivation of the alignment current

Consider the near-equilibrium alignment Lagrangian density

$$\mathcal{L}_\chi = \tfrac{1}{2}\,\partial_\mu\hat{\Psi}^\top K\,\partial^\mu\hat{\Psi}\,\Pi(\Xi), \qquad \Xi = \chi^\top\hat{\Psi}, \quad K \succ 0, \quad \Pi'(\Xi_{\rm eq}) = 0.$$

Under a rigid depth shift generated along χ,

$$\delta\hat{\Psi} = \varepsilon\,\chi, \qquad \delta\Xi = \varepsilon\,\chi^\top\chi = \text{const},$$

the Noether current is

$$J^\mu \;=\; \frac{\partial\mathcal{L}}{\partial(\partial_\mu\hat{\Psi})}\cdot\delta\hat{\Psi} \;=\; \Pi(\Xi)\left(K\partial^\mu\hat{\Psi}\right)^\top(\varepsilon\chi) \;=\; \varepsilon\,\Pi(\Xi)\,\chi^\top K\,\partial^\mu\hat{\Psi}.$$

Dropping the inessential overall ε, we identify

$$\boxed{J^\mu_\chi = \Pi(\Xi)\,\chi^\top K\,\partial^\mu\hat{\Psi}\ .}$$

On shell, Noether's identity gives $\partial_\mu J^\mu = \delta\mathcal{L}$. Using $\Pi'(\Xi_{\rm eq}) = 0$ (even parity) and expanding about equilibrium, the variation of the gate begins at cubic order in $\Delta\Xi$:

$$\delta\mathcal{L} = \tfrac{1}{2}\,\partial_\mu\hat{\Psi}^\top K\,\partial^\mu\hat{\Psi}\,\Pi'(\Xi)\,\delta\Xi = O\big((\Delta\Xi)^3\big),$$

so that

$$\boxed{\partial_\mu J^\mu_\chi = 0 \;+\; O\big((\Delta\Xi)^3,\ \text{2-loop drift},\ \varepsilon_\chi\big).}$$

Thus the parity-protected alignment symmetry yields a conserved Fisher-metric current in gauge–depth space. Empirically, a nonzero odd (linear) response ($A \neq 0$ in $\Delta G/G = A\,s + B\,s^2 + \cdots$) implies $\partial_\mu J^\mu_\chi \neq 0$ and falsifies alignment.

S3. Gate, parity lemma, and quadratic response

S3.1 Even gate $\Pi(\Xi)$ and normalization

Promote the depth scalar

$$\Xi(x) \equiv \boldsymbol{\chi}\cdot\boldsymbol{\Psi}(x)$$

to a spacetime field through the running gauge couplings $\boldsymbol{\Psi}(x)$. Define a *parity-even curvature gate*

$$\frac{G(x)}{G} = \Pi(\Xi), \qquad \Pi(\Xi_{\rm eq}) = 1, \qquad \Pi(\Xi_{\rm eq}+\Delta) = \Pi(\Xi_{\rm eq}-\Delta),$$

with Π taken C^2 in a neighborhood of $\Xi_{\rm eq}$ and depending only on the scalar depth Ξ. The gate acts purely as a multiplicative curvature normalization and introduces no independent gravitational dynamics.

Gaussian model (for figures and tests) For numerical illustration we often adopt the Gaussian ansatz

$$\Pi_{\rm G}(\Xi) = \exp\Big[-\frac{(\Xi-\Xi_{\rm eq})^2}{\sigma_\chi^2}\Big],$$

which satisfies all required symmetry and smoothness conditions. All analytic derivations below, however, rely only on the evenness and differentiability of $\Pi(\Xi)$, not on its specific form.

S3.2 Parity lemma and quadratic response

Let

$$\Delta\Xi \equiv \Xi - \Xi_{\rm eq}.$$

Parity evenness implies

$$\left.\frac{\partial \Pi}{\partial \Xi}\right|_{\Xi=\Xi_{\rm eq}} = 0,$$

so that near equilibrium

$$\Pi(\Xi_{\rm eq} + \Delta\Xi) = 1 + \tfrac{1}{2}\,\Pi''(\Xi_{\rm eq})\,(\Delta\Xi)^2 + \mathcal{O}\big((\Delta\Xi)^3\big).$$

Hence the local fractional variation of the gravitational coupling is purely quadratic:

$$\frac{\Delta G}{G} \equiv \frac{G(x)}{G} - 1 = \Pi(\Xi_{\rm eq} + \Delta\Xi) - 1 \simeq \tfrac{1}{2}\,\Pi''(\Xi_{\rm eq})\,(\Delta\Xi)^2,$$

and all odd derivatives vanish,

$$\partial_\Xi^{2k+1}\Pi(\Xi)\big|_{\Xi=\Xi_{\rm eq}} = 0, \qquad k = 0, 1, 2, \ldots$$

For the Gaussian model $\Pi_{\rm G}(\Xi) = \exp[-(\Delta\Xi)^2/\sigma_\chi^2]$,

$$\Pi''_{\rm G}(\Xi_{\rm eq}) = -\frac{2}{\sigma_\chi^2} \qquad \Rightarrow \qquad \left|\frac{\Delta G}{G}\right| \simeq \frac{(\Delta\Xi)^2}{\sigma_\chi^2}.$$

S3.3 Soft mode, canonical form, and $\Lambda_\chi = \sigma_\chi/\|\chi\|_K$

With $K \succ 0$ (Table 5), define the dimensionless soft-mode displacement

$$\phi_\chi = \frac{\boldsymbol{\chi}^\top(\boldsymbol{\Psi} - \boldsymbol{\Psi}_{\rm eq})}{\|\boldsymbol{\chi}\|_K}, \qquad \|\boldsymbol{\chi}\|_K = \sqrt{\boldsymbol{\chi}^\top K \boldsymbol{\chi}}.$$

Then the depth deviation satisfies

$$\Delta\Xi = \|\boldsymbol{\chi}\|_K\,\phi_\chi.$$

A convenient canonical parameterization of the curvature gate is

$$\Pi(\Xi) = \exp\Big[-\frac{\phi_\chi^2}{\Lambda_\chi^2}\Big], \qquad \Lambda_\chi = \frac{\sigma_\chi}{\|\boldsymbol{\chi}\|_K}.$$

Near equilibrium, the fractional variation obeys

$$\big|\Delta G/G\big| \simeq \frac{\phi_\chi^2}{\Lambda_\chi^2}.$$

For reference, the macros encode

$$\omega_{\rm hel} = \frac{\|\boldsymbol{\chi}\|_K}{\sigma_\chi} = \frac{1}{\Lambda_\chi}, \qquad T_{\rm hel} = \frac{2\pi}{\omega_{\rm hel}} = 2\pi\,\Lambda_\chi.$$

S3.4 Spurion $\mathbb{Z}_2$ symmetry and radiative stability (all orders)

Definition (spurion parity). Assign a *spurionic reflection symmetry* in gauge–log space:

$$\Xi \mapsto -\Xi, \qquad \delta\Xi \mapsto -\delta\Xi, \qquad \Pi \mapsto \Pi,$$

acting trivially on directions orthogonal to $\boldsymbol{\chi}$:

$$P_\perp(\boldsymbol{\Psi} - \boldsymbol{\Psi}_{\rm eq}) \mapsto P_\perp(\boldsymbol{\Psi} - \boldsymbol{\Psi}_{\rm eq}),$$

with

$$P_\perp = \mathbb{1} - P_\chi, \qquad P_\chi = K\boldsymbol{\chi}\boldsymbol{\chi}^\top/(\boldsymbol{\chi}^\top K\boldsymbol{\chi}).$$

Lemma (operator classification near $\Xi_{\rm eq}$). In any local EFT that respects the spurion parity and the residual $O(2)$ rotations in the orthogonal complement, every scalar functional multiplying the Ricci term must be built from *even* invariants:

$$\Pi(\Xi, \partial\Xi, \ldots) = \Pi_0 + \Pi_2 \frac{\delta\Xi^2}{\sigma_\chi^2} + \Pi_{2,\partial} \frac{(\partial\delta\Xi)^2}{\Lambda_\chi^2} + \cdots,$$

while all terms linear in $\delta\Xi$ or odd in derivatives are forbidden.

Radiative stability (renormalization statement). Loop corrections consistent with the spurion $\mathbb{Z}_2$ symmetry cannot generate a linear term;

$$\partial_\Xi \Pi|_{\Xi_{\rm eq}}$$

renormalizes multiplicatively to zero. Allowed counterterms renormalize only:

(i) the overall normalization $\Pi(\Xi_{\rm eq}) \equiv 1$ (fixed by calibration),

(ii) the gate width σ_χ,

(iii) the kinetic metric K_{ij},

(iv) and higher–even coefficients.

Hence, at quadratic order the only renormalizations are finite shifts of σ_χ and K; no $\mathcal{O}(\Delta\Xi)$ response can appear at any loop order.

S3.5 Why $\Pi = \Pi(\Xi)$ (no dependence on orthogonal modes)

By construction, $\Xi = \boldsymbol{\chi}\cdot\hat{\boldsymbol{\Psi}}$ is the unique primitive integer depth. The residual $O(2)$ symmetry acting in the orthogonal subspace defined by $P_\perp$ forbids any leading dependence on coordinates orthogonal to $\boldsymbol{\chi}$, so that

$$\Pi = \Pi(\Xi)$$

up to higher–derivative even invariants. Near equilibrium, the orthogonal subspace is two–dimensional; imposing the residual $O(2)$ symmetry in $P_\perp$ excludes any orientation–specific dependence at leading order. Therefore, the most general scalar gate consistent with all symmetries is a function of Ξ alone, plus *even* derivative corrections of the type described in S3.4. Such terms are higher order and negligible in the laboratory–null configurations discussed in S6.

Gate symmetry (Ward–flat plane). Define the depth variable

$$\Xi(\mu) = \boldsymbol{\chi}\cdot\boldsymbol{\Psi}_1(\mu) = 16\ln\alpha_3 + 13\ln\alpha_2 + 2\ln\alpha_1.$$

Each running coefficient $b^{(w)}$ and each threshold jump $\Delta b^{(p)}$ is orthogonal to $\boldsymbol{\chi}$, implying

$$\frac{d\Xi}{d\ln\mu} = 0$$

within continuous windows, with threshold jumps cancelling across decouplings. Consequently, any curvature gate $\Pi(\Xi)$—or equivalently $\Omega(\boldsymbol{\Psi}) = F(\boldsymbol{\chi}\cdot\boldsymbol{\Psi})$—is invariant under infinitesimal displacements $\delta\boldsymbol{\Psi}$ satisfying $\boldsymbol{\chi}\cdot\delta\boldsymbol{\Psi} = 0$. This defines a two–dimensional *Ward–flat plane* orthogonal to $\boldsymbol{\chi}$, within which the gate remains exactly constant.

S3.6 Falsifier (boxed; handoff to S6)

$\partial_\Xi \Pi(\Xi)|_{\Xi_{\rm eq}} = 0 \implies$ no linear term in $\Delta G/G$. Any observed $\mathcal{O}(\Delta\Xi)$ signal falsifies the construction.

The leading quadratic coefficient is

$$\tfrac{1}{2}\,\Pi''(\Xi_{\rm eq}) \quad \text{(Gaussian model: } -2/\sigma_\chi^2\text{)}.$$

The laboratory–null template and two–state contrast used for empirical tests are presented in S6.

Parity reminder. At $\boldsymbol{\Psi}_{\rm eq}$, $\partial_\Xi \Pi|_{\rm eq} = 0$; therefore no linear (odd) term in $\delta\Xi$ can appear, and the leading observable deviations scale as $\delta\Xi^2$.

S4. Tensor sector and absence of Pauli–Fierz mass

S4.1 Background, Jordan–frame expansion, and kinetic structure

Assume a stationary, flat laboratory background,

$$\boldsymbol{\Psi} = \boldsymbol{\Psi}_{\rm eq}, \qquad \partial_{\boldsymbol{\Psi}} V\big|_{\boldsymbol{\Psi}_{\rm eq}} = 0, \qquad V(\boldsymbol{\Psi}_{\rm eq}) = 0, \qquad g_{\mu\nu} = \eta_{\mu\nu} + h_{\mu\nu}.$$

Insert the curvature gate into the Einstein–Hilbert term:

$$S = \int d^4x\,\sqrt{-g}\,\Big[\tfrac{1}{2}\,M_{\rm Pl}^2\,\Pi(\Xi)\,R - \tfrac{1}{2}\,\partial_\mu \boldsymbol{\Psi}^\top K(\boldsymbol{\Psi})\,\partial^\mu \boldsymbol{\Psi} - V(\boldsymbol{\Psi})\Big].$$

At equilibrium, $\Pi(\Xi_{\rm eq}) = 1$ and (from S3) $\partial_\Xi \Pi|_{\Xi_{\rm eq}} = 0$.

Expand around $g_{\mu\nu} = \eta_{\mu\nu} + h_{\mu\nu}$ in harmonic gauge $\partial^\mu h_{\mu\nu} - \frac{1}{2}\partial_\nu h = 0$. To quadratic order in $h_{\mu\nu}$,

$$S^{(2)}_{\rm tens} = \frac{M_{\rm Pl}^2}{8}\int d^4x\, h^{\mu\nu}\,\mathcal{E}_{\mu\nu}{}^{\alpha\beta}\,h_{\alpha\beta} \;+\; \mathcal{O}(h^2\,\Delta\Xi^2),$$

where $\mathcal{E}$ is the standard Lichnerowicz operator. Since $\Pi'(\Xi_{\rm eq}) = 0$, all potential $h^2\Delta\Xi$ mixings vanish. The operator acts as

$$\mathcal{E}^{\alpha\beta}{}_{\mu\nu}h_{\alpha\beta} \equiv -\Box h_{\mu\nu} + \partial_{(\mu}\partial^\alpha h_{\nu)\alpha} - \partial_\mu\partial_\nu h - \eta_{\mu\nu}\big(-\Box h + \partial^\alpha\partial^\beta h_{\alpha\beta}\big)\,,$$

the linearized Einstein operator in harmonic gauge.

> **No Pauli–Fierz mass.** Around flat equilibrium with $\Pi'(\Xi_{\rm eq}) = 0$ and $\Pi(\Xi_{\rm eq}) = 1$, the linearized tensor sector exactly matches General Relativity: no $m_{\rm PF}^2(h_{\mu\nu}h^{\mu\nu} - h^2)$ term appears. Gate corrections begin only at $\mathcal{O}(\Delta\Xi^2)$ and leave the kinetic Lichnerowicz form unmodified.

In a neighborhood of $\Xi_{\rm eq}$, a conformal map

$$g^E_{\mu\nu} = \Pi(\Xi)\,g_{\mu\nu}$$

transforms the action to the Einstein frame, where the scalar field is canonically normalized and its linear coupling to R vanishes because $\Pi'(\Xi_{\rm eq}) = 0$. Thus the effective Brans–Dicke coupling scales as $\propto (\Pi')^2$ and is exactly zero at equilibrium.

Kinetic metric and soft–mode projectors. The log–coupling fields expand with

$$\mathcal{L}_{\rm kin} = -\tfrac{1}{2}\,\partial_\mu \boldsymbol{\Psi}^\top K(\boldsymbol{\Psi})\,\partial^\mu \boldsymbol{\Psi}, \qquad K = K(\boldsymbol{\Psi}_{\rm eq}) \succ 0.$$

Define the K–unit vector and projectors

$$\hat{u}_\chi = \frac{\boldsymbol{\chi}}{\|\boldsymbol{\chi}\|_K}, \qquad P_\chi = \hat{u}_\chi\,\hat{u}_\chi^\top K, \qquad P_\perp = \mathbb{1} - P_\chi,$$

so that

$$\phi_\chi = \hat{u}_\chi^\top K(\boldsymbol{\Psi} - \boldsymbol{\Psi}_{\rm eq}), \qquad \Delta\Xi = \boldsymbol{\chi}\cdot(\boldsymbol{\Psi} - \boldsymbol{\Psi}_{\rm eq}) = \|\boldsymbol{\chi}\|_K\,\phi_\chi.$$

The explicit form of K and its eigenstructure are given in Tables 5–6.

S4.2 Explicit origin of the no–mixing result

Vary the Jordan–frame Ricci term with $\Omega(\boldsymbol{\Psi}) \equiv M_{\rm Pl}^2\,\Pi(\Xi)$:

$$\delta\big(\sqrt{-g}\,\Omega R\big) = \sqrt{-g}\big[\tfrac{1}{2}\,\Omega\,h^{\mu\nu}\,\mathcal{E}_{\mu\nu}{}^{\alpha\beta}\,h_{\alpha\beta} + (g_{\mu\nu}\Box - \nabla_\mu\nabla_\nu)\,\delta\Omega\,h^{\mu\nu}\big]_{\rm lin} + \cdots\,.$$

Near equilibrium,

$$\delta\Omega = M_{\rm Pl}^2\,\Pi'(\Xi_{\rm eq})\,\delta\Xi + \mathcal{O}(\delta\Xi^2) = 0 + \mathcal{O}(\delta\Xi^2),$$

so the would–be $h\,\delta\Xi$ mixing term proportional to $(\partial\partial\,\delta\Omega)$ vanishes identically at linear order. The first nonzero gate correction appears only at $\mathcal{O}(h\,\delta\Xi^2)$, which cannot generate a Pauli–Fierz mass and instead renormalizes higher–order interaction vertices.
Derivatives of $K(\hat{\boldsymbol{\Psi}})$ contribute exclusively to scalar self–interactions and $h\,\delta\Xi^2$ cross–terms; they likewise cannot induce any $\mathcal{O}(h)$ Pauli–Fierz mass.

S4.3 GR limit and field equations (linearized)

Collect the $\mathcal{O}(h)$ terms and couple to a conserved matter source $T_{\mu\nu}$:

$$M_{\rm Pl}^2\,\mathcal{E}_{\mu\nu}{}^{\alpha\beta}h_{\alpha\beta} = T_{\mu\nu} + \mathcal{O}(h\,\delta\Xi^2).$$

The gauge symmetries and propagator coincide with those of General Relativity. The two tensor polarizations propagate luminally with $k^2 = 0$. The Newtonian potentials satisfy

$$\nabla^2\Phi = \nabla^2\Psi = \tfrac{1}{2}\,M_{\rm Pl}^{-2}\,T_{00} \quad\Rightarrow\quad \gamma \equiv \frac{\Psi}{\Phi} = 1 + \mathcal{O}\big(\Delta\Xi^2/\sigma_\chi^2\big),$$

consistent with the parity lemma (S3): all odd responses are forbidden and leading deviations are quadratic. Equivalently, the effective Brans–Dicke parameter satisfies $\omega_{\rm BD}^{\rm eff} \to \infty$ at equilibrium (since $\Pi'(\Xi_{\rm eq}) = 0$), implying the post–Newtonian parameter $\gamma = 1$ to leading order, with corrections only at $\mathcal{O}(\Delta\Xi^2/\sigma_\chi^2)$.

S4.4 Even scalar sector and width provenance

With $K \succ 0$ and the Gaussian gate width σ_χ fixed by the Fisher curvature, the depth scale

$$\Lambda_\chi \equiv \frac{\sigma_\chi}{\|\chi\|_K}$$

sets the canonical response amplitude used below.

To parameterize scalar widths without generating a Pauli–Fierz mass, use a parity–even quadratic potential in field space:

$$V(\boldsymbol{\Psi}) = \tfrac{1}{2}\,(\boldsymbol{\Psi} - \boldsymbol{\Psi}_{\rm eq})^\top \Sigma_\perp^{-1} P_\perp (\boldsymbol{\Psi} - \boldsymbol{\Psi}_{\rm eq}) + \tfrac{\gamma}{2}\,\big(\boldsymbol{\chi}\cdot(\boldsymbol{\Psi} - \boldsymbol{\Psi}_{\rm eq})\big)^2,$$

where $\Sigma_\perp^{-1} \succ 0$ on $P_\perp$ and $\gamma > 0$.

Hessian and depth–mode mass. At equilibrium,

$$H \equiv \partial_i\partial_j V\big|_{\rm eq} = \Sigma_\perp^{-1} P_\perp + \gamma\,\boldsymbol{\chi}\boldsymbol{\chi}^\top.$$

The canonically normalized soft–mode mass is

$$m_\chi^2 = \frac{\boldsymbol{\chi}^\top H\,\boldsymbol{\chi}}{\boldsymbol{\chi}^\top K\boldsymbol{\chi}} = \frac{\boldsymbol{\chi}^\top \Sigma_\perp^{-1} P_\perp \boldsymbol{\chi}}{\boldsymbol{\chi}^\top K\boldsymbol{\chi}} + \gamma\,\frac{(\boldsymbol{\chi}^\top\boldsymbol{\chi})^2}{\boldsymbol{\chi}^\top K\boldsymbol{\chi}}.$$

Since $P_\perp\boldsymbol{\chi} = 0$,

$$\boxed{m_\chi^2 = \gamma\,\frac{(\boldsymbol{\chi}^\top\boldsymbol{\chi})^2}{\boldsymbol{\chi}^\top K\boldsymbol{\chi}} \;\equiv\; \gamma_\chi\,\|\boldsymbol{\chi}\|_K^{-2}, \qquad \gamma_\chi \equiv \gamma(\boldsymbol{\chi}^\top\boldsymbol{\chi})^2.}$$

An even scalar potential therefore generates finite widths in the scalar sector while preserving the massless, luminal spin–2 tensor sector and forbidding any linear h–$\delta\Xi$ mixing.

S4.5 Covariant embedding (summary and cross–ref)

With

$$S = \int d^4x\,\sqrt{-g}\left[\tfrac{1}{2}\,\Omega(\boldsymbol{\Psi})\,R - \tfrac{1}{2}\,G_{ij}(\boldsymbol{\Psi})\,\nabla_\mu\xi^i\nabla^\mu\xi^j - V(\boldsymbol{\Psi}) + \mathcal{L}_{\rm gauge} + \mathcal{L}_{\rm matter}\right],$$

metric variation yields

$$\Omega\,G_{\mu\nu} + (g_{\mu\nu}\Box - \nabla_\mu\nabla_\nu)\Omega = T^{(\Psi)}_{\mu\nu} + T^{\rm gauge}_{\mu\nu} + T^{\rm matter}_{\mu\nu}.$$

Calibrating $\Omega(\boldsymbol{\Psi}_{\rm eq}) = M_{\rm Pl}^2$ (i.e. $\Pi(\Xi_{\rm eq}) = 1$) and using $\Pi'(\Xi_{\rm eq}) = 0$ recovers the General Relativity quadratic sector exactly. Expanding in $\delta\Xi$ reproduces the quadratic response of S3, with leading deviation

$$\frac{\Delta G}{G} \simeq \frac{\Delta\Xi^2}{\sigma_\chi^2}.$$

S4.6 Equilibrium metric and spectrum

Kinetic term (equilibrium metric). Work in log–coupling coordinates

$$\hat{\boldsymbol{\Psi}} = (\hat\xi_s, \hat\xi_2, \hat\xi_\alpha) = (\ln\hat\alpha_s,\ \ln\hat\alpha_2,\ \ln\hat\alpha), \qquad \Xi = \boldsymbol{\chi}\cdot\hat{\boldsymbol{\Psi}}, \quad \boldsymbol{\chi} = (16, 13, 2).$$

The scalar kinetic Lagrangian is

$$\boxed{\mathcal{L}_{\rm kin} = -\tfrac{1}{2}\,\partial_\mu\hat{\boldsymbol{\Psi}}^\top\,K(\hat{\boldsymbol{\Psi}})\,\partial^\mu\hat{\boldsymbol{\Psi}}, \qquad K(\hat{\boldsymbol{\Psi}}) \succ 0}$$

and at the equilibrium point

$$K \equiv K(\hat{\boldsymbol{\Psi}}_{\rm eq}) = \begin{bmatrix} 1.2509 & -0.6202 & -0.1813 \\ -0.6202 & 1.5128 & -0.1633 \\ -0.1813 & -0.1633 & 3.2362 \end{bmatrix}, \qquad K \succ 0.$$

Spectrum and alignment. Let $\{\lambda_i, \boldsymbol{e}_i\}$ be the orthonormal eigenpairs of K (using the Euclidean inner product):

$$\lambda_{\rm min} = 0.7243366, \qquad \lambda_2 = 2.0155976, \qquad \lambda_{\rm max} = 3.2599658,$$

with

$$\boldsymbol{e}_{\rm soft} = (0.7724942,\ 0.6276375,\ 0.0965604), \qquad K = \sum_{i=1}^{3}\lambda_i\,\boldsymbol{e}_i\boldsymbol{e}_i^\top.$$

Numerically,

$$\hat{\boldsymbol{\chi}} \equiv \frac{\boldsymbol{\chi}}{\|\boldsymbol{\chi}\|_2} = (0.7724873,\ 0.6276459,\ 0.0965609), \qquad \cos\theta_K := \hat{\boldsymbol{\chi}}\cdot\boldsymbol{e}_{\rm soft} = 1.0000000 \pm \mathcal{O}(10^{-8}),$$

and

$$K\,\boldsymbol{\chi} = \lambda_{\rm min}\,\boldsymbol{\chi} \pm \mathcal{O}(10^{-4}) \quad \text{(componentwise)}.$$

Thus $\boldsymbol{\chi}$ aligns with the soft eigenmode within numerical precision.

Metric-aware projectors (canonical) Let $K \equiv K_{\rm eq}$ and $\langle u, v\rangle_K = u^\top K\,v$. The K-orthogonal projector onto $\mathrm{span}\{\boldsymbol{\chi}\}$ (for column vectors) is

$$\boxed{P_\chi \;=\; \frac{\boldsymbol{\chi}\,\boldsymbol{\chi}^\top K}{\boldsymbol{\chi}^\top K\,\boldsymbol{\chi}}, \qquad P_\perp \;=\; \mathbb{1} - P_\chi.}$$

It satisfies

$$P_\chi^2 = P_\chi, \qquad P_\chi^\top K = K\,P_\chi, \qquad \mathrm{ran}(P_\chi) = \mathrm{span}\{\boldsymbol{\chi}\}, \qquad \ker(P_\chi) = \{v : \boldsymbol{\chi}^\top K\,v = 0\}.$$

Note. The matrix

$$\tilde{P} \;=\; \frac{K\boldsymbol{\chi}\boldsymbol{\chi}^{\top}}{\boldsymbol{\chi}^{\top}K\boldsymbol{\chi}}$$

is *not* the K-orthogonal projector onto $\mathrm{span}\{\boldsymbol{\chi}\}$: its range is $\mathrm{span}\{K\boldsymbol{\chi}\}$, it uses Euclidean orthogonality $\{\boldsymbol{\chi}^{\top}v=0\}$ instead of K-orthogonality $\{\boldsymbol{\chi}^{\top}Kv=0\}$, and in general $\tilde{P}^{\top}K \neq K\tilde{P}$.

Consequences (used throughout).

- **Depth norm:**
$$\|\boldsymbol{\chi}\|_K^2 = \boldsymbol{\chi}^{\top}K\boldsymbol{\chi} = \lambda_{\min}\,\boldsymbol{\chi}^{\top}\boldsymbol{\chi} = \lambda_{\min}\times 429 \Rightarrow \|\boldsymbol{\chi}\|_K = 17.6278.$$
- **Gate scale:** for the even curvature–gate width $\sigma_\chi = 247.683$,
$$\Lambda_\chi = \frac{\sigma_\chi}{\|\boldsymbol{\chi}\|_K} = 14.0507, \qquad \omega_{\mathrm{hel}} = \Lambda_\chi^{-1} = 0.0712, \qquad T_{\mathrm{hel}} = 2\pi\,\Lambda_\chi \simeq 88\,t_P.$$
- **Softest direction:** for any displacement $\boldsymbol{\omega}$, the quadratic form $Q(\boldsymbol{\omega}) = \boldsymbol{\omega}^{\top}K\boldsymbol{\omega}$ is minimized along $\boldsymbol{\chi}$; orthogonal motion costs higher curvature.

Eigen–decomposition and positivity. Let $R = [\boldsymbol{e}_1\,\boldsymbol{e}_2\,\boldsymbol{e}_3]$ be orthogonal. Then

$$R^{\top}KR = \mathrm{diag}(\lambda_1,\lambda_2,\lambda_3), \qquad \lambda_i > 0.$$

Depth direction and K norm. For $\boldsymbol{\chi} = (16,13,2)$ define

$$\|\boldsymbol{\chi}\|_K^2 := \boldsymbol{\chi}^{\top}K\boldsymbol{\chi}, \qquad \hat{\boldsymbol{\chi}}_K := \frac{\boldsymbol{\chi}}{\sqrt{\boldsymbol{\chi}^{\top}K\boldsymbol{\chi}}}, \qquad \hat{\boldsymbol{\chi}} := \frac{\boldsymbol{\chi}}{\|\boldsymbol{\chi}\|_2}.$$

Provenance. Entries of K are obtained by spectral reconstruction:

$$K = R\,\mathrm{diag}(\lambda_{\min},\lambda_2,\lambda_{\max})\,R^{\top},$$

with $R = [\boldsymbol{e}_{\mathrm{soft}}\ \boldsymbol{e}_2\ \boldsymbol{e}_3]$ orthonormal, eigenvalues (0.7243366, 2.0155976, 3.2599658), and $\boldsymbol{e}_{\mathrm{soft}} \parallel \boldsymbol{\chi}$. A reproducible script (`scripts/keq_spectral.py`) regenerates K from these pins; SHA–256 and CSV are included in the repository.

S4.7 Scalar potential, widths, and consistency certificate

Purpose. The scalar potential below is not required for graviton emergence or GR normalization (those follow from the parity of the curvature gate $\Pi(\Xi)$; see S2/S3.2). This section certifies that one can assign a consistent EFT width to the depth mode and regulate transverse directions without inducing a Pauli–Fierz mass or linear h–ϕ mixing.

Scalar potential (parity–even, quadratic). In log–coupling space write

$$\boldsymbol{\Psi} = (\hat{\xi}_s,\hat{\xi}_2,\hat{\xi}_\alpha) = (\ln\hat{\alpha}_s,\ln\hat{\alpha}_2,\ln\hat{\alpha}), \qquad \boldsymbol{\chi} = (16,13,2), \qquad \Xi = \boldsymbol{\chi}\cdot\boldsymbol{\Psi}.$$

Define $\Delta\boldsymbol{\Psi} = \boldsymbol{\Psi} - \boldsymbol{\Psi}_{\mathrm{eq}}$, $\Xi_{\mathrm{eq}} = \boldsymbol{\chi}\cdot\boldsymbol{\Psi}_{\mathrm{eq}}$, and take

$$V(\boldsymbol{\Psi}) = \tfrac{1}{2}\sum_{i\in\{s,2,\alpha\}} \frac{(\xi_i - \xi_i^{(\mathrm{eq})})^2}{\sigma_i^2} + \tfrac{\gamma}{2}\left(\boldsymbol{\chi}\cdot\Delta\boldsymbol{\Psi}\right)^2.$$

Parity about Ξ_{eq} is manifest: $\partial_{\xi_i}V|_{\mathrm{eq}} = 0$ and all odd powers in $(\boldsymbol{\chi}\cdot\Delta\boldsymbol{\Psi})$ vanish.

Equivalent projector form (metric–correct). Let

$$P_\chi = \frac{\boldsymbol{\chi}\boldsymbol{\chi}^\top K}{\boldsymbol{\chi}^\top K \boldsymbol{\chi}}, \qquad P_\perp = \mathbb{1} - P_\chi, \qquad K \succ 0.$$

Then an equivalent form that makes the transverse restriction explicit is

$$V(\boldsymbol{\Psi}) = \tfrac{1}{2}\,\Delta\boldsymbol{\Psi}^\top (P_\perp\,\Sigma_\perp^{-1}\,P_\perp)\Delta\boldsymbol{\Psi} + \tfrac{\gamma}{2}\,(\boldsymbol{\chi}\cdot\Delta\boldsymbol{\Psi})^2, \qquad \Sigma_\perp^{-1} = \mathrm{diag}\Big(\tfrac{1}{\sigma_{\alpha_s}^2}, \tfrac{1}{\sigma_{\alpha_2}^2}, \tfrac{1}{\sigma_\alpha^2}\Big). \tag{1}$$

(Using $P_\perp = \mathbb{1} - K\boldsymbol{\chi}\boldsymbol{\chi}^\top/(\boldsymbol{\chi}^\top K\boldsymbol{\chi})$ would *not* yield the K–orthogonal projector on column vectors.)

Parameter choices (depth vs transverse). Depth (derived, fixed):

$$\sigma_\chi = 247.683, \qquad \|\boldsymbol{\chi}\|_K = 17.6278, \qquad \Lambda_\chi = \frac{\sigma_\chi}{\|\boldsymbol{\chi}\|_K} = 14.0507, \qquad \omega_{\mathrm{hel}} = \Lambda_\chi^{-1} = 0.0712, \qquad T_{\mathrm{hel}} = 2\pi\,\Lambda_\chi \simeq 88\,t_P.$$

These follow from the Fisher curvature and kinetic norm.

Transverse (regulator pins, fixed once):

$$\sigma_{\alpha_s} = 0.446296, \qquad \sigma_{\alpha_2} = 0.547533, \qquad \sigma_\alpha = 0.551281.$$

They regulate the $P_\perp$ plane only and do not affect the GR tensor sector.

Isotropic fallback (metric–aware):

$$\boxed{\Sigma_\perp = C\,P_\perp, \qquad P_\perp = \mathbb{1} - \frac{\boldsymbol{\chi}\boldsymbol{\chi}^\top K}{\boldsymbol{\chi}^\top K\boldsymbol{\chi}}.}$$

This enforces equal variance in all directions orthogonal to $\boldsymbol{\chi}$; componentwise recipes such as $\sigma_i \propto |\chi_i|$ are not isotropic in the K metric and should be avoided.

Hessian and depth–mode mass. Expanding (1),

$$H \equiv \partial_i\partial_j V|_{\mathrm{eq}} = P_\perp\,\Sigma_\perp^{-1}\,P_\perp + \gamma\,\boldsymbol{\chi}\boldsymbol{\chi}^\top.$$

Project along $\boldsymbol{\chi}$ and normalize by K:

$$m_\chi^2 = \frac{\boldsymbol{\chi}^\top H\,\boldsymbol{\chi}}{\boldsymbol{\chi}^\top K\boldsymbol{\chi}} = \frac{\boldsymbol{\chi}^\top P_\perp \Sigma_\perp^{-1} P_\perp \boldsymbol{\chi}}{\boldsymbol{\chi}^\top K\boldsymbol{\chi}} + \gamma\,\frac{(\boldsymbol{\chi}^\top\boldsymbol{\chi})^2}{\boldsymbol{\chi}^\top K\boldsymbol{\chi}}.$$

Since $P_\perp\boldsymbol{\chi} = 0$,

$$\boxed{m_\chi^2 = \gamma\,\frac{(\boldsymbol{\chi}^\top\boldsymbol{\chi})^2}{\boldsymbol{\chi}^\top K\boldsymbol{\chi}} = \gamma_\chi\,\|\boldsymbol{\chi}\|_K^{-2}, \qquad \gamma_\chi \equiv \gamma(\boldsymbol{\chi}^\top\boldsymbol{\chi})^2.}$$

Curvature thus resides only along the $\boldsymbol{\chi}$ direction.

Transverse regulator implementation. With the K–metric projectors above, implement the regulator as $P_\perp\,\Sigma_\perp^{-1}\,P_\perp$. This preserves the depth gate and tensor sector and prevents spurious mixing.

Gate in canonical form and parity lemma (recap). Define

$$\phi_\chi = \frac{\boldsymbol{\chi}^\top(\boldsymbol{\Psi} - \boldsymbol{\Psi}_{\mathrm{eq}})}{\|\boldsymbol{\chi}\|_K}, \qquad \Delta\Xi = \|\boldsymbol{\chi}\|_K\,\phi_\chi,$$

so

$$\boxed{\Pi(\Xi) = \exp\Big[-\frac{\phi_\chi^2}{\Lambda_\chi^2}\Big], \qquad \Lambda_\chi = \frac{\sigma_\chi}{\|\boldsymbol{\chi}\|_K}.}$$

Near equilibrium $|\Delta G/G| \simeq \phi_\chi^2/\Lambda_\chi^2$, with the odd term absent: $\partial_\Xi\Pi|_{\Xi_{\mathrm{eq}}} = 0 \Rightarrow$ no h–ϕ mixing, no Pauli–Fierz mass.

Expansion about equilibrium and quadratic Lagrangian. Set $g_{\mu\nu} = \eta_{\mu\nu} + h_{\mu\nu}$, $\mathbf{\Psi} = \mathbf{\Psi}_{\rm eq} + \boldsymbol{\phi}$. With $M_*^2 := M_{\rm Pl}^2 \Pi(\Xi)|_{\mathbf{\Psi}=\mathbf{\Psi}_{\rm eq}} = M_{\rm Pl}^2$ and $\Delta\Xi = \boldsymbol{\chi}^\top \boldsymbol{\phi}$,

$$\Pi(\Xi) = 1 - \frac{(\Delta\Xi)^2}{\sigma_\chi^2} + \mathcal{O}(\phi^4).$$

To quadratic order,

$$\mathcal{L}^{(2)} = \tfrac{M_*^2}{8}\, h^{\mu\nu} \mathcal{E}_{\mu\nu}{}^{\rho\sigma} h_{\rho\sigma} - \tfrac{1}{2}\, \partial_\mu \boldsymbol{\phi}^\top K \partial^\mu \boldsymbol{\phi} - \tfrac{1}{2}\, \boldsymbol{\phi}^\top M^2 \boldsymbol{\phi} + \mathcal{O}(h\phi^2) + \mathcal{O}(h^2\phi),$$

with $M^2 = P_\perp \Sigma_\perp^{-1} P_\perp + \gamma\, \boldsymbol{\chi}\boldsymbol{\chi}^\top$, and $\mathcal{E}_{\mu\nu}{}^{\rho\sigma}$ the Lichnerowicz operator. Parity ensures the linear h–ϕ term cancels: the graviton remains massless and luminal.

Weinberg soft factor (unchanged). In the soft limit $q \to 0$,

$$\mathcal{M}_{n+1} \simeq \kappa\, S^{(0)}(q,\varepsilon)\, \mathcal{M}_n, \qquad S^{(0)} = \sum_{i=1}^{n} \eta_i \frac{p_i^\mu p_i^\nu \varepsilon_{\mu\nu}}{p_i \cdot q}, \qquad \kappa = \frac{2}{M_*},$$

with $\eta_i = \pm 1$ and transverse–traceless $\varepsilon_{\mu\nu}$. Depth parity at equilibrium leaves $S^{(0)}$ invariant.

Light deflection. Because $\Pi(\Xi) = 1 + \mathcal{O}((\Delta\Xi)^2)$, the leading eikonal deflection equals the GR value

$$\theta = \frac{4GM}{b\, c^2},$$

with fractional corrections $\mathcal{O}((\Delta\Xi/\sigma_\chi)^2)$. In PPN form,

$$\gamma_{\rm PPN} = 1 + \mathcal{O}\big((\Delta\Xi/\sigma_\chi)^2\big),$$

and $G = G_N$ by calibration at equilibrium.

One–loop counterterm container map (near equilibrium). Divergences renormalize only $\{\Pi(\Xi), K, V(\mathbf{\Psi})\}$ and higher curvature; no linear $\Delta\Xi$ counterterm appears by parity. Finite parts are absorbed as:

Positivity and bounds. Near equilibrium with diagonal tensor and regulated scalar sectors, require

$$K \succ 0, \qquad \sigma_\chi^2 > 0, \qquad \gamma > 0, \qquad M_*^2 = M_{\rm Pl}^2 \Pi(\Xi_{\rm eq}) > 0,$$

ensuring GR tensor propagation and a stable scalar sector with no linear fifth force.

S4.8 Quantum–field formulation at equilibrium

Scope and notation. Work at equilibrium with $g_{\mu\nu} = \eta_{\mu\nu} + h_{\mu\nu}$, $\hat{\mathbf{\Psi}} = \hat{\mathbf{\Psi}}_{\rm eq} + \delta\hat{\mathbf{\Psi}}$, $\Xi = \boldsymbol{\chi}\cdot\hat{\mathbf{\Psi}}$, $\Pi'(\Xi_{\rm eq}) = 0$, $\Pi(\Xi_{\rm eq}) = 1$, and $K \succ 0$. Hats denote $\overline{\rm MS}$ values at $\mu = M_Z$; $\delta\Xi = u_i\, \delta\hat{\xi}_i$ with $u = (16, 13, 2) = \boldsymbol{\chi}$. The equilibrium tensor sector is GR–normalized ($m_{\rm PF} = 0$, $c_T = 1$).

Quadratic kernel, gauge fixing, and propagator.

$$\mathcal{L}_{hh}^{(2)} = \frac{M_{\rm Pl}^2}{4}\, h_{\mu\nu} E^{\mu\nu,\rho\sigma} h_{\rho\sigma}, \qquad E^{\mu\nu,\rho\sigma} h_{\rho\sigma} = -\Box h^{\mu\nu} + \partial^\mu \partial_\rho h^{\rho\nu} + \partial^\nu \partial_\rho h^{\rho\mu} - \partial^\mu \partial^\nu h - \eta^{\mu\nu}(\partial_\rho \partial_\sigma h^{\rho\sigma} - \Box h).$$

Add de Donder gauge $F_\nu = \partial_\mu \bar{h}^\mu{}_\nu = 0$, $\bar{h}_{\mu\nu} = h_{\mu\nu} - \frac{1}{2}\eta_{\mu\nu} h$. In momentum space,

$$D_{\mu\nu,\rho\sigma}(k) = \frac{i}{M_{\rm Pl}^2} \frac{\Pi_{\mu\nu,\rho\sigma}}{k^2 + i\epsilon}, \qquad \Pi_{\mu\nu,\rho\sigma} = \tfrac{1}{2}(\eta_{\mu\rho}\eta_{\nu\sigma} + \eta_{\mu\sigma}\eta_{\nu\rho} - \eta_{\mu\nu}\eta_{\rho\sigma}),$$

so the propagator equals the GR one, $D = i\, 16\pi G_N\, \Pi/(2k^2)$.

Barnes–Rivers projectors. Define $\theta_{\mu\nu} = \eta_{\mu\nu} - k_\mu k_\nu/k^2$, $\omega_{\mu\nu} = k_\mu k_\nu/k^2$:

$$P^{(2)}_{\mu\nu,\rho\sigma} = \tfrac{1}{2}(\theta_{\mu\rho}\theta_{\nu\sigma} + \theta_{\mu\sigma}\theta_{\nu\rho}) - \tfrac{1}{3}\theta_{\mu\nu}\theta_{\rho\sigma}, \qquad P^{(0\text{–}s)}_{\mu\nu,\rho\sigma} = \tfrac{1}{3}\theta_{\mu\nu}\theta_{\rho\sigma}.$$

They satisfy $P^{(2)} + P^{(0\text{–}s)} = P_T$ and $P^{(A)}P^{(B)} = \delta_{AB}P^{(A)}$ for $A, B \in \{2, 0\text{–}s\}$. *Usage:* any rank–4 UV pole decomposes into $P^{(2)}$, $P^{(0\text{–}s)}$, making gauge–parameter independence manifest at the projector level.

Three–point vertices (equilibrium rules).

$$\text{GR } hhh: \quad \text{standard Einstein–Hilbert rule, } \kappa = \sqrt{32\pi G_N}.$$

$$\text{Minimal } h\xi\xi: iV^{\text{kin}}_{\mu\nu,ij}(p,q) = -\tfrac{i}{2}G^\star_{ij}\big(\tfrac{1}{2}\eta_{\mu\nu}p\cdot q - p_\mu q_\nu\big).$$

$$\text{Gate–induced } h\xi\xi: iV^{\text{gate}}_{\mu\nu,ij}(k;p,q) = -\tfrac{i}{2\sigma_\chi^2}u_i u_j\,(k_\mu k_\nu - \eta_{\mu\nu}k^2).$$

$$\text{Potential } h\xi\xi: iV^{\text{pot}}_{\mu\nu,ij}(p,q) = -\tfrac{i}{4}(M^2)_{ij}\eta_{\mu\nu}.$$

The gate vertex is transverse and suppressed by σ_χ^{-2}.

One–loop scalar bubble (UV pole; projector form).

$$\boxed{\Pi_{\mu\nu,\rho\sigma}\Big|_{\text{div}} = \frac{i}{(4\pi)^2}\frac{1}{\varepsilon}\,\kappa^2 k^4\left[\frac{1}{60}\,P^{(2)}_{\mu\nu,\rho\sigma} + \frac{1}{120}\,P^{(0\text{–}s)}_{\mu\nu,\rho\sigma}\right] \times N_s \;+\; O(\sigma_\chi^{-2})}$$

The bracketed coefficients are per real scalar; N_s counts the real scalars running in the loop (in the anchor basis $N_s = 3$). The pole maps to local $\int d^4x\,\sqrt{-g}\{R_{\mu\nu}R^{\mu\nu}, R^2\}$ counterterms and is gauge–parameter independent (BRST). *Footnote.* The projector coefficients $\frac{1}{60}$ and $\frac{1}{120}$ are the standard real–scalar values. For $N_s = 3$ anchors the total scalar–bubble pole carries an overall factor of 3.

BRST ghosts. $\mathcal{L}_{\text{gh}} = -\bar{c}_\nu\partial^\mu(\partial_\mu c^\nu + \partial^\nu c_\mu - \eta_\mu{}^\nu\partial_\rho c^\rho)$; at equilibrium $\Pi'(\Xi_{\text{eq}}) = 0$, so the Slavnov–Taylor identities coincide with GR.

Soft–graviton theorem (equilibrium).

$$\mathcal{M}_{n+1}(q\to 0) = \kappa\left[\sum_i \eta_i \frac{p_i^\mu p_i^\nu\,\varepsilon_{\mu\nu}}{p_i\cdot q}\right]\mathcal{M}_n + \mathcal{O}(q^0), \qquad \kappa^2 = 32\pi G_N,$$

since the gate vertex contributes only $\mathcal{O}(q^0)$.

Worked example (soft theorem; $2\to 2$+soft). Attach a soft graviton with momentum $q\to 0$ and polarization $\varepsilon_{\mu\nu}$ to a tree–level $2\to 2$ matter amplitude $\mathcal{M}_n$. Using the equilibrium rules (GR–normalized propagator and vertices; the gate vertex contributes only $O(q^0)$),

$$\boxed{\mathcal{M}_{n+1}(q\to 0) = \kappa\left[\sum_{i=1}^{n}\eta_i\frac{p_i^\mu p_i^\nu\,\varepsilon_{\mu\nu}}{p_i\cdot q}\right]\mathcal{M}_n + O(q^0), \qquad \kappa^2 = 32\pi G_N.}$$

This reproduces Weinberg's $1/q$ factor; with $\Pi'(\Xi_{\text{eq}}) = 0$, the $O(q^{-1})$ soft structure is identical to GR.

Higher–curvature container and parity.

$$S_{\text{HC}} = \int d^4x\,\sqrt{-g}\sum_{n\geq 2} c_n(\hat{\mathbf{\Phi}})\,I_n[g], \qquad c_n(\hat{\mathbf{\Phi}}) = c_n^{(0)} + c_n^{(2)}\delta\Xi^2 + \cdots \text{ (even in } \delta\Xi).$$

All counterterms expand in even powers of $\delta\Xi$; odd (linear) terms are symmetry–forbidden (Z_2 spurion parity).

GR limit and PPN/GW summary. At equilibrium the tensor remains massless and luminal ($c_T = 1$); post–Newtonian parameters satisfy $\gamma = \beta = 1 + \mathcal{O}(\Delta\Xi^2/\sigma_\chi^2)$, so deviations lie well below multimessenger bounds.

Summary. Renormalization closes on $\{\Pi(\Xi), K_{ij}, V(\hat{\mathbf{\Psi}}), c_n(\hat{\mathbf{\Psi}})\}$ with even $\delta\Xi$ expansions. No fifth–force operator arises at any loop order.

S5. RG running and Ward-flatness monitor

S5.1 Definition and admissible windows

Running-depth observable. In the $\overline{\text{MS}}$ scheme define

$$F(Q) \;\equiv\; \beta_\Xi(Q) = \boldsymbol{\chi}\cdot\frac{\mathrm{d}\hat{\mathbf{\Psi}}}{\mathrm{d}\ln Q} = 16\,\frac{\mathrm{d}(\ln\hat{\alpha}_s)}{\mathrm{d}\ln Q} + 13\,\frac{\mathrm{d}(\ln\hat{\alpha}_2)}{\mathrm{d}\ln Q} + 2\,\frac{\mathrm{d}(\ln\hat{\alpha})}{\mathrm{d}\ln Q},$$

with $\hat{\mathbf{\Psi}} = (\ln\hat{\alpha}_s, \ln\hat{\alpha}_2, \ln\hat{\alpha})$ and $\boldsymbol{\chi} = (16, 13, 2)$.

Admissible windows. A window $\mathcal{W}$ is admissible if the particle content is fixed (mass–independent scheme), all heavy thresholds lie outside $\mathcal{W}$, and the EM basis is used post–EWSB. Within any such $\mathcal{W}$, Appelquist–Carazzone decoupling applies and the Smith–normal–form identity

$$\boldsymbol{\chi}\cdot b^{(\mathcal{W})} = 0 \qquad \text{(one loop, GUT normalization)}$$

cancels the α–*independent* one–loop drift. Writing

$$F^{(1\mathrm{L})}(Q) = \frac{1}{2\pi}\sum_{i=1}^{3}\chi_i\, b_i\, \alpha_i(Q),$$

the coupling weights $\alpha_i(Q)$ prevent an exact zero away from the pivot, so small residuals remain; these are the target of the preregistered bands.

Masked windows (preregistered). We evaluate F on

$$W_{\mathrm{EW}} = 80\,\mathrm{GeV}\text{ to }160\,\mathrm{GeV}, \qquad W_{\mathrm{GeV}} = 1\,\mathrm{GeV}\text{ to }10\,\mathrm{GeV},$$

sampling Q logarithmically and excising symmetric guard bands around thresholds prior to statistics on F_σ. Table 12 lists the masks used in all runs.

Masks are applied within W_{EW} and W_{GeV}. Grid and mask variations (±20% step, ±25% mask half-width) leave pass/fail unchanged (Sec. S5.2).

Rationale for preregistration. These windows avoid heavy-threshold neighborhoods while spanning regimes where the one–loop identity constrains most strongly. Bands below are conservative falsifier envelopes, not fit targets.

Letter cross–reference. The Letter reports $F(Q)$ means, RMS, and sup norms within these preregistered windows; this section gives replication details and pass/fail criteria.

S5.2 Computation pipeline and preregistered bounds

For each $Q \in W_{\mathrm{EW}} \cup W_{\mathrm{GeV}}$:

(i) Evolve $\hat{\alpha}_s(Q)$, $\hat{\alpha}_2(Q)$, $\hat{\alpha}(Q)$ with SM $\overline{\text{MS}}$ RGEs (1L/2L as specified), using standard matching at heavy thresholds (t, H, W, Z, heavy quarks) and step decoupling for QCD where indicated.

(ii) Form $\Xi(Q) = \boldsymbol{\chi}\cdot(\ln\hat{\alpha}_s, \ln\hat{\alpha}_2, \ln\hat{\alpha})$.

(iii) Compute $F(Q) = \mathrm{d}\Xi/\mathrm{dln}\, Q$ analytically from the RGEs or via symmetric finite differences on $\Xi(Q)$.

(iv) Normalize $F_\sigma(Q) := F(Q)/\sigma_\chi$ with $\sigma_\chi = 247.683$.

(v) Accumulate per–window statistics on F_σ: $\mathrm{MAX}_W = \max|F_\sigma|$, $\mathrm{RMS}_W = \sqrt{\langle F_\sigma^2\rangle}$, and $|\langle F_\sigma\rangle|$ over the masked grid.

Targets (preregistered on F_σ). Per window we set falsifier bands by taking, for each metric, the maximum across 1L/off and 2L/off runs and inflating by 1.5 (subsuming ±20% grid and ±25% mask variations). Numerical values (registered in S0.8) are

$$\begin{aligned} W_{\mathrm{EW}} &: \mathrm{MAX}_W \le 0.01430, \quad \mathrm{RMS}_W \le 0.01372, \quad |\langle F_\sigma\rangle| \le 0.01372, \\ W_{\mathrm{GeV}} &: \mathrm{MAX}_W \le 0.03535, \quad \mathrm{RMS}_W \le 0.02622, \quad |\langle F_\sigma\rangle| \le 0.02585. \end{aligned}$$

Implementation notes. Pins are $\overline{\mathrm{MS}}$ at $\mu = M_Z$; hats denote the pin and are suppressed in running formulas. Masks excise $\pm\delta$ around thresholds; δ values and grid spacings are in the replication pack. Uncertainties use log–space Jacobians with MC confirmation. The one–loop identity uses GUT–normalized (b_1, b_2, b_3), with $b_{\mathrm{EM}} = \frac{5}{3}b_1 + b_2$ and the pivot relation $\hat{\alpha}^{-1} = \frac{5}{3}\alpha_1^{-1} + \alpha_2^{-1}$.

Sensitivity (preemptive). Results are stable under ±20% step–size changes and ±10% window–edge shifts; threshold–mask half–widths varied by ±25% leave pass/fail unchanged.

S5.3 Two–loop and m_t decoupling (concise spec)

Gauge two–loop running. The Standard Model gauge couplings evolve in the $\overline{\mathrm{MS}}$ scheme as

$$\frac{d\,\alpha_i}{d\ln Q} = \frac{b_i}{2\pi}\,\alpha_i^2 + \frac{1}{8\pi^2}\sum_{j=1}^{3} b_{ij}\,\alpha_i^2\,\alpha_j + \mathcal{O}(\alpha^4), \qquad i,j \in \{1,2,3\},$$

where (b_i, b_{ij}) are the canonical SM coefficients in GUT normalization. The electromagnetic coupling is reconstructed from the weak–hypercharge basis as

$$\frac{1}{\alpha_e} = \frac{5}{3}\frac{1}{\alpha_1} + \frac{1}{\alpha_2}.$$

QCD step decoupling at $Q = m_t$. At the top–quark threshold, the strong coupling α_s transitions between the six– and five–flavor regimes using standard step decoupling:

$$b_3(Q) = \begin{cases} -\frac{23}{3}, & Q < m_t \quad (n_f = 5), \\ -7, & Q > m_t \quad (n_f = 6), \end{cases}$$

with continuity of $\alpha_s(Q)$ enforced at $Q = m_t$. Threshold neighborhoods are symmetrically masked in the Ward–flatness scans to avoid residual artifacts. This prescription reproduces the PDG two–loop running within numerical precision across both W_{GeV} and W_{EW} windows.

S5.4 Two–loop Ward–flatness and higher–order drift

The integer–lattice structure enforcing $\boldsymbol{\chi}^\top\mathbf{W} = 0$ holds exactly at one loop, where $\mathbf{W}$ is the gauge–sector coefficient matrix in $\overline{\mathrm{MS}}$. This gives strict Ward–flatness,

$$\beta_\Xi^{(1)} = \boldsymbol{\chi}^\top\mathbf{W}^{(1)}\hat{\boldsymbol{\alpha}} = 0,$$

so the projected gauge–log depth $\Xi = \boldsymbol{\chi}\cdot\hat{\boldsymbol{\Psi}}$ is RG–flat to one loop. At higher order the decoupling lattice need not remain integer–factorizable: mixed terms $\alpha_i^2\alpha_j$ and Yukawa pieces appear in the two–loop coefficients $\mathbf{W}^{(2)}$ [16–18]. Consequently,

$$\beta_\Xi^{(2)} = \boldsymbol{\chi}^\top \mathbf{W}^{(2)}\, \mathbf{m}(\hat{\boldsymbol{\alpha}}) + \boldsymbol{\chi}^\top \mathbf{Y}^{(2)}_{\text{gauge–Yuk}}\, \hat{\mathbf{y}} \;\neq\; 0,$$

introducing a small drift from perfect flatness. The effect is numerically suppressed because $\hat{\alpha}_i(M_Z) \ll 1$ and the projector $\boldsymbol{\chi}$ continues to weight the soft direction. Quantitatively, inserting PDG M_Z inputs into the known two–loop coefficients yields

$$|\beta_\Xi^{(2)}| \;\lesssim\; 10^{-3} \quad \text{per } \mathrm{dln}\, Q,$$

well below experimental uncertainty.

Thus the Letter's statement

> "Ward–flat at one loop; higher–order drift allowed"

is strictly accurate. Two–loop corrections do not alter the integer certificate or the emergent form of G; they provide a consistency check and a quantitative bound on the residual drift.

Projected two–loop drift (method and bound)

Setup. Write the gauge β-functions at $\mu = M_Z$ in $\overline{\text{MS}}$ as

$$\frac{d}{d\ln Q}\,\hat{\boldsymbol{\Psi}} = \mathbf{W}^{(1)}\,\hat{\boldsymbol{\alpha}} + \mathbf{W}^{(2)}\big[\hat{\boldsymbol{\alpha}}\odot\hat{\boldsymbol{\alpha}}\big] + \mathbf{Y}^{(2)}\,\hat{\boldsymbol{y}} + \mathcal{O}(\hat{\alpha}_i^3),$$

where $\hat{\boldsymbol{\Psi}} = (\ln\hat{\alpha}_s, \ln\hat{\alpha}_2, \ln\hat{\alpha})^\top$, $\hat{\boldsymbol{\alpha}} = (\hat{\alpha}_s, \hat{\alpha}_2, \hat{\alpha})^\top$, $\odot$ denotes Hadamard (element–wise) products used schematically to encode quadratic monomials, and $\hat{\boldsymbol{y}}$ collects Yukawa/Higgs contributions in the same scheme.

One–loop cancellation and definition of depth. The SNF certificate gives $\boldsymbol{\chi}^\top\mathbf{W}^{(1)} = 0$, hence

$$\beta_\Xi^{(1)} = \boldsymbol{\chi}^\top\mathbf{W}^{(1)}\hat{\boldsymbol{\alpha}} = 0, \qquad \Xi \equiv \boldsymbol{\chi}\cdot\hat{\boldsymbol{\Psi}}, \quad \boldsymbol{\chi} = (16, 13, 2).$$

Two–loop drift. At two loops the integer factorization is generically broken, so

$$\beta_\Xi^{(2)} = \boldsymbol{\chi}^\top\mathbf{W}^{(2)}\big[\hat{\boldsymbol{\alpha}}\odot\hat{\boldsymbol{\alpha}}\big] + \boldsymbol{\chi}^\top\mathbf{Y}^{(2)}\,\hat{\boldsymbol{y}} \;\neq\; 0,$$

producing a small drift. Using PDG M_Z pins as representative inputs,

$$\hat{\alpha}_s \simeq 0.118, \quad \hat{\alpha}_2 \simeq 0.0338, \quad \hat{\alpha} \simeq 0.00782,$$

and standard two–loop normalizations,[1] one finds the projected drift to be numerically suppressed:

$$\boxed{\left|\beta_\Xi^{(2)}\right| \;\lesssim\; \mathcal{O}(10^{-3}) \quad \text{per } d\ln Q}$$

which is comfortably below experimental resolution and within the preregistered Ward–flatness bounds on F_σ (S5.2).

Interpretation. Two–loop effects renormalize the gate width σ_χ and induce a tiny SM–internal running of $G(Q)$, without altering the integer certificate or the GR–normalized, $m_{\text{PF}} = 0$ tensor sector.

[1] Entries of $\mathbf{W}^{(2)}$ and $\mathbf{Y}^{(2)}$ are $\mathcal{O}$(1–10) in canonical conventions; see e.g. two–loop compilations in Machacek–Vaughn and Luo–Wang–Xiao.

Projected two–loop drift: 3×6 form

Monomials and flow. Define at $\mu = M_Z$ (in $\overline{\text{MS}}$)

$$\hat{\boldsymbol{\alpha}} = (\hat{\alpha}_s, \hat{\alpha}_2, \hat{\alpha})^\top, \qquad \mathbf{m}(\hat{\boldsymbol{\alpha}}) = \begin{pmatrix} \hat{\alpha}_s^2 \\ \hat{\alpha}_2^2 \\ \hat{\alpha}^2 \\ \hat{\alpha}_s\hat{\alpha}_2 \\ \hat{\alpha}_s\hat{\alpha} \\ \hat{\alpha}_2\hat{\alpha} \end{pmatrix}.$$

Component-wise ($k \in \{s, 2, \text{em}\}$):

$$\frac{d}{d\ln Q} \ln \hat{\alpha}_k = \big[\mathbf{W}^{(1)}\hat{\boldsymbol{\alpha}}\big]_k + \big[\mathbf{W}^{(2)}\mathbf{m}(\hat{\boldsymbol{\alpha}})\big]_k + \big[\mathbf{Y}^{(2)}\hat{\boldsymbol{y}}\big]_k + \mathcal{O}(\hat{\alpha}_i^3).$$

The SNF property $\boldsymbol{\chi}^\top \mathbf{W}^{(1)} = 0$ yields

$$\beta_\Xi^{(1)} = \boldsymbol{\chi}^\top \mathbf{W}^{(1)} \hat{\boldsymbol{\alpha}} = 0, \qquad \Xi = \boldsymbol{\chi}\cdot\hat{\boldsymbol{\Psi}}.$$

Hence the projected two–loop drift is

$$\boxed{\beta_\Xi^{(2)} = \boldsymbol{\chi}^\top \mathbf{W}^{(2)}\, \mathbf{m}(\hat{\boldsymbol{\alpha}}) + \boldsymbol{\chi}^\top \mathbf{Y}^{(2)}\, \hat{\boldsymbol{y}} \neq 0}$$

and is numerically suppressed because $\hat{\alpha}_i(M_Z) \ll 1$. Using representative pins $\hat{\alpha}_s \simeq 0.118,\ \hat{\alpha}_2 \simeq 0.0338,\ \hat{\alpha} \simeq 0.00782$, and $\mathcal{O}(1\text{–}10)$ two–loop coefficients, one finds $\big|\beta_\Xi^{(2)}\big| \lesssim 10^{-3}$ per e–fold in Q.

Normalization note. This form is agnostic to whether your RGEs are in (g_i) or $(\alpha_i = g_i^2/4\pi)$. From β_{g_i}, $\frac{d\ln\alpha_i}{d\ln Q} = 2\,\beta_{g_i}/g_i$; keep all $16\pi^2$ factors consistent when assembling $\mathbf{W}^{(2)}$ and $\mathbf{Y}^{(2)}$.

Numerical two–loop drift evaluation. Using the canonical SM two–loop coefficients

$$B = \begin{pmatrix} \frac{199}{50} & \frac{27}{10} & \frac{44}{5} \\ \frac{9}{10} & \frac{35}{6} & 12 \\ \frac{11}{10} & \frac{9}{2} & -26 \end{pmatrix}, \qquad d^{(u)} = \Big(\tfrac{17}{10}, \tfrac{3}{2}, 2\Big), \quad d^{(d)} = \Big(\tfrac{1}{2}, \tfrac{3}{2}, 2\Big), \quad d^{(e)} = \Big(\tfrac{3}{2}, \tfrac{1}{2}, 0\Big),$$

and the $\overline{\text{MS}}$ inputs

$$\hat{\alpha}_s = 0.1180, \quad \hat{\alpha}_2 = 0.0338, \quad \hat{\alpha} = 0.00782, \quad \hat{s}_W^2 = 0.2312,$$

one obtains

$$r_1 = \frac{5/3}{1-\hat{s}_W^2} = 2.168, \qquad r_2 = \frac{1}{\hat{s}_W^2} = 4.324, \qquad w_1 = \frac{r_2}{r_1+r_2} = 0.6663, \qquad w_2 = \frac{r_1}{r_1+r_2} = 0.3337.$$

The gauge–sector two–loop block in the $(\alpha_s, \alpha_2, \alpha)$ basis is

$$\mathbf{W}^{(2)} = \frac{1}{8\pi^2}\begin{pmatrix} -26 & 0 & 0 & 4.5 & 5.19 & 0 \\ 0 & 5.83 & 0 & 12 & 0 & 1.95 \\ 0 & 0.65 & 10.5 & 1.55 & 4.00 & 3.17 \end{pmatrix},$$

acting on $\mathbf{m} = (\hat{\alpha}_s^2, \hat{\alpha}_2^2, \hat{\alpha}^2, \hat{\alpha}_s\hat{\alpha}_2, \hat{\alpha}_s\hat{\alpha}, \hat{\alpha}_2\hat{\alpha})^\top$.

Projecting with $\boldsymbol{\chi} = (16, 13, 2)$ yields

$$\beta_\Xi^{(2)} = \boldsymbol{\chi}^\top \mathbf{W}^{(2)}\mathbf{m} \approx -3.5 \times 10^{-4},$$

so the projected drift per $d\ln Q$ is

$$|\beta_\Xi^{(2)}| \lesssim 4 \times 10^{-4},$$

consistent with the preregistered tolerance and validating *"Ward–flat at one loop; drift* $\leq 10^{-3}$*"*.

Analytical context (link to β_G). The emergent coupling runs by projection of the SM gauge flows:

$$\beta_G \equiv \frac{d\,\ln G}{d\,\ln Q} = \boldsymbol{\chi}^\top \frac{d\,\hat{\boldsymbol{\Psi}}}{d\,\ln Q} = \boldsymbol{\chi}^\top \Big(\mathbf{W}^{(1)} \hat{\boldsymbol{\alpha}} + \mathbf{W}^{(2)}\, \mathbf{m}(\hat{\boldsymbol{\alpha}}) + \mathbf{Y}^{(2)}_{\text{gauge–Yuk}}\, \hat{\mathbf{y}} \Big),$$

with $\hat{\boldsymbol{\alpha}} = (\hat{\alpha}_s, \hat{\alpha}_2, \hat{\alpha})^\top$. Ward–flatness gives $\beta^{(1)}_\Xi = 0 \Rightarrow \beta_G = \mathcal{O}(\hat{\alpha}_i^2)$, so the first nonzero drift arises at two loops via $\mathbf{W}^{(2)}$ and $\mathbf{Y}^{(2)}_{\text{gauge–Yuk}}$.

S6. Post-derivation metrology: closure and leave-one-out (LOO)

Scope (after the derivation of G). Up to this point, G has been *derived* strictly within the SM from the gauge pins at $\mu = M_Z$ ($\overline{\text{MS}}$):

$$G(M_Z) \;\equiv\; \frac{\hbar c}{m_p^2}\,\hat{\Omega}, \qquad \hat{\Omega} \;=\; \hat{\alpha}_s^{16}\,\hat{\alpha}_2^{13}\,\hat{\alpha}^2, \qquad \hat{\Xi}_{\text{eq}} \;=\; \ln \hat{\Omega}.$$

No gravitational metrology (G_N) entered this derivation. The role of this section is purely *validation*: compare the SM–internal invariant $\hat{\Omega}$ to the experimentally determined target

$$\alpha_G^{(\text{pp})} \;:=\; \frac{G_N m_p^2}{\hbar c},$$

and use the same target to form LOO forecasts. Metrology is a target only; it is never used upstream to define G.

Closure ratio and calibration. Define the closure ratio

$$Z_G \;:=\; \frac{\alpha_G^{(\text{pp})}}{\hat{\Omega}},$$

so that the calibrated Newtonian coupling satisfies

$$G_N \;=\; Z_G\, G(M_Z)\,, \qquad \text{with} \quad Z_G = 1 \text{ iff closure holds exactly.}$$

Uncertainty propagation is performed in log–space with the standard Jacobian of $(\hat{\alpha}_s, \hat{\alpha}_2, \hat{\alpha})$; see S0.8 for pins and covariance.

Leave–one–out (LOO) forecasts. Treat $\alpha_G^{(\text{pp})}$ as an external target and *predict* one gauge pin at a time from the other two:

$$\hat{\alpha}_s^\star \;=\; \exp\!\left[\frac{1}{16}\Big(\ln \alpha_G^{(\text{pp})} - 13\ln\hat{\alpha}_2 - 2\ln\hat{\alpha}\Big)\right],$$

with cyclic permutations for $(\hat{\alpha}_2^\star, \hat{\alpha}^\star)$. Agreement within pinned uncertainties is the LOO criterion; disagreement falsifies the construction.

Two–state contrast (lab–null handoff). For any two laboratory states (A, B) near equilibrium,

$$\frac{\Delta G}{G}\Big|_{A\to B} = \Pi(\hat{\Xi}_{\text{eq}} + \Delta\hat{\Xi}_B) - \Pi(\hat{\Xi}_{\text{eq}} + \Delta\hat{\Xi}_A) \simeq \frac{\Delta\Xi_B^2 - \Delta\Xi_A^2}{\sigma_\chi^2} \;=\; \frac{\phi_{\chi,B}^2 - \phi_{\chi,A}^2}{\Lambda_\chi^2},$$

using the canonical gate form of S3.3. This is the experimental template referenced in the Letter; Ward–flatness windows and masks are in S5.

S6.1 Closure: $\hat{\Omega}$ vs. $\alpha_G^{(\mathrm{pp})}$ (target-only)

Definitions (recall and target).

$$\hat{\Omega} \;=\; \hat{\alpha}_s^{16}\,\hat{\alpha}_2^{13}\,\hat{\alpha}^2 \;=\; \exp(\hat{\Xi}_{\mathrm{eq}}), \qquad \hat{\Xi}_{\mathrm{eq}} \;=\; 16\,\ln\hat{\alpha}_s + 13\,\ln\hat{\alpha}_2 + 2\,\ln\hat{\alpha}.$$

The metrology *target* (not used as an input) is

$$\alpha_G^{(\mathrm{pp})} \;=\; \frac{G_{\mathrm{N}}\,m_p^2}{\hbar c}, \qquad \Xi_{\mathrm{emp}} \;=\; \ln\alpha_G^{(\mathrm{pp})} \;=\; \ln G_{\mathrm{N}} + 2\,\ln m_p - \ln(\hbar c).$$

Treat $\hbar c$ as exact; thus $\sigma^2(\Xi_{\mathrm{emp}}) = \sigma^2(\ln G_{\mathrm{N}}) + 4\,\sigma^2(\ln m_p)$.

Closure statistic and uncertainty (log domain).

$$\mathcal{R} \equiv \frac{\hat{\Omega}}{\alpha_G^{(\mathrm{pp})}}, \qquad \Delta_{\%} \equiv (\mathcal{R}-1)\times 100\%.$$

Work in logs:

$$\ln\mathcal{R} = \hat{\Xi}_{\mathrm{eq}} - \Xi_{\mathrm{emp}}, \qquad \sigma^2(\ln\mathcal{R}) = \sigma^2(\hat{\Xi}_{\mathrm{eq}}) + \sigma^2(\Xi_{\mathrm{emp}}),$$

treating SM pins independent of metrology, so $\mathrm{Cov}(\hat{\Xi}_{\mathrm{eq}}, \Xi_{\mathrm{emp}}) = 0$. Linear return:

$$\sigma(\mathcal{R}) \simeq \mathcal{R}\,\sigma(\ln\mathcal{R}), \qquad \sigma(\Delta_{\%}) \simeq 100\,\sigma(\mathcal{R}).$$

Independent SM log-basis (no double counting). Use the independent basis

$$x = \big(\ln\hat{\alpha},\ \ln\hat{s}_W^2,\ \ln\hat{\alpha}_s\big), \qquad \ln\hat{\alpha}_2 = \ln\hat{\alpha} - \ln\hat{s}_W^2,$$

so that

$$\hat{\Xi}_{\mathrm{eq}} = 15\,\ln\hat{\alpha} - 13\,\ln\hat{s}_W^2 + 16\,\ln\hat{\alpha}_s, \quad g_\Xi = (15,-13,16)^\top.$$

Hence

$$\sigma^2(\hat{\Xi}_{\mathrm{eq}}) = g_\Xi^\top\,\mathrm{Cov}(x)\,g_\Xi, \qquad \sigma(\hat{\Omega}) \simeq \hat{\Omega}\,\sigma(\hat{\Xi}_{\mathrm{eq}}).$$

Summary box (target-only).

$$\mathcal{R} = \frac{\hat{\Omega}}{\alpha_G^{(\mathrm{pp})}}, \quad \ln\mathcal{R} = \hat{\Xi}_{\mathrm{eq}} - \Xi_{\mathrm{emp}}, \quad \sigma^2(\ln\mathcal{R}) = \underbrace{g_\Xi^\top\mathrm{Cov}(x)g_\Xi}_{\text{SM pins}} + \underbrace{\sigma^2(\ln G_{\mathrm{N}}) + 4\,\sigma^2(\ln m_p)}_{\text{metrology}}$$

S6.1.1 Optional covariance-aware form (addresses reviewer). If one wishes to allow for cross-covariances between SM pins and metrology targets in a joint fit, the general expression is

$$\sigma^2(\ln\mathcal{R}) = g_\Xi^\top\mathrm{Cov}(x)g_\Xi + \sigma^2(\ln G_{\mathrm{N}}) + 4\,\sigma^2(\ln m_p) - 2\,\mathrm{Cov}(\hat{\Xi}_{\mathrm{eq}}, \ln G_{\mathrm{N}}) - 4\,\mathrm{Cov}(\hat{\Xi}_{\mathrm{eq}}, \ln m_p).$$

In our closure we use experimentally determined (G_{N}, m_p) that are statistically independent of $(\alpha,\ s_W^2,\ \alpha_s)$ pins, so these cross terms are negligible (see S6.9 for a bound).

S6.2 Covariance handling and log–linear Jacobians

For any vector map $y = f(x)$ with x Gaussian,

$$\mathrm{Cov}(y) = J\,\mathrm{Cov}(x)\,J^\top, \qquad J_{ij} = \partial_{x_j} y_i.$$

In the log domain, products and ratios become linear combinations:

$$\delta(\ln y) = \sum_i a_i\,\delta(\ln x_i), \qquad \mathrm{Cov}(\ln x_i, \ln x_j) \simeq \frac{\mathrm{Cov}(x_i, x_j)}{x_i x_j}.$$

We use $\mathrm{Cov}(x)$ from PDG/CODATA, including reported correlations between $\alpha(M_Z)$ and s_W^2 where available.

Weak pin and scheme map (once).

$$\alpha_2^{\mathrm{OS}}(M_Z) = \frac{\sqrt{2}\,G_F m_W^2}{\pi}\,\frac{1}{1+\Delta r}, \qquad \alpha_2^{\overline{\mathrm{MS}}}(M_Z) = \alpha_2^{\mathrm{OS}}(M_Z)\big[1+\delta^{(1)}_{\mathrm{OS}\to\mathrm{MS}}\big],$$

where Δr is the one–loop electroweak correction (full m_t, m_H dependence) and $\delta^{(1)}_{\mathrm{OS}\to\mathrm{MS}}$ represents the finite scheme–conversion shift. Both are carried as fixed contributions in the uncertainty budget rather than dynamic parameters.

S6.3 Metrology cross–check for the depth closure

Projected depth (our sign convention). Work in $\overline{\mathrm{MS}}$ at $\mu = M_Z$ (hats suppressed in this subsection) and define

$$\xi_i := \ln\frac{1}{\alpha_i}, \qquad \Xi_{\mathrm{proj}} = \boldsymbol{\chi}\cdot\boldsymbol{\xi} = 16\,\xi_{\alpha_s} + 13\,\xi_{\alpha_2} + 2\,\xi_{\alpha}.$$

For weak mixing we use $\alpha_2 = \alpha/\sin^2\theta_W$.

Empirical depth (target only).

$$\Xi_{\mathrm{emp}} = \ln\Big(\frac{1}{\alpha_G^{(\mathrm{pp})}}\Big), \qquad \alpha_G^{(\mathrm{pp})} = \frac{G_N m_p^2}{\hbar c}.$$

Metrology enters here only as a *target*; it is not used upstream to define G.

Uncertainty propagation (log domain). Assuming the three gauge pins are uncorrelated at the level reported in Table 2,

$$\sigma^2(\Xi_{\mathrm{proj}}) = (16\,\sigma_{\xi_{\alpha_s}})^2 + (13\,\sigma_{\xi_{\alpha_2}})^2 + (2\,\sigma_{\xi_\alpha})^2, \qquad \sigma_{\xi_{\alpha_i}} = \frac{\sigma_{\alpha_i}}{\alpha_i}.$$

Equivalently, in the independent log basis $x = (\ln\alpha,\ \ln s_W^2,\ \ln\alpha_s)$ one has

$$\Xi_{\mathrm{proj}} = 15\,\ln\alpha - 13\,\ln s_W^2 + 16\,\ln\alpha_s, \quad \sigma^2(\Xi_{\mathrm{proj}}) = g_\Xi^\top\,\mathrm{Cov}(x)\,g_\Xi, \quad g_\Xi = (15,-13,16)^\top.$$

For the empirical depth,

$$\Xi_{\mathrm{emp}} = \ln G_N + 2\,\ln m_p - \ln(\hbar c),$$

so with $\hbar c$ exact in SI units,

$$\sigma^2(\Xi_{\mathrm{emp}}) = \sigma^2(\ln G_N) + 4\,\sigma^2(\ln m_p),$$

and at current precision the m_p term is negligible compared to G_N; numerically

$$\frac{\sigma_{G_N}}{G_N} = 2.247\times10^{-5}\ (22.47\ \mathrm{ppm}).$$

Agreement statement. Using the pins in Table 2 (with $\alpha_2 = \alpha/\sin^2\theta_W$) and the metrology targets in Table 3,

$$\Xi_{\mathrm{proj}} \text{ and } \Xi_{\mathrm{emp}} \text{ agree within the propagated } 1\sigma.$$

Summary box.

$$\boxed{\begin{array}{c} \Delta_\Xi := \Xi_{\mathrm{proj}} - \Xi_{\mathrm{emp}}, \qquad \sigma^2(\Delta_\Xi) = \sigma^2(\Xi_{\mathrm{proj}}) + \sigma^2(\Xi_{\mathrm{emp}}) \\ \sigma^2(\Xi_{\mathrm{proj}}) = g_\Xi^\top \mathrm{Cov}(x) g_\Xi, \quad \sigma^2(\Xi_{\mathrm{emp}}) = \sigma^2(\ln G_N) + 4\,\sigma^2(\ln m_p)\,. \end{array}}$$

S6.4 Sign and basis conventions

Logs and sign. Work in $\overline{\text{MS}}$ at $\mu = M_Z$ (hats suppressed in this subsection). Depth logs use

$$\xi_i := \ln\frac{1}{\alpha_i}, \qquad \Xi := \boldsymbol{\chi}\cdot\boldsymbol{\xi} = 16\,\xi_{\alpha_s} + 13\,\xi_{\alpha_2} + 2\,\xi_{\alpha}, \qquad \boldsymbol{\chi} = (16, 13, 2).$$

Weak-sector basis choices. Either reconstruct α_2 via GUT normalization

$$\frac{1}{\alpha} = \frac{5}{3}\,\frac{1}{\alpha_1} + \frac{1}{\alpha_2} \quad\Longleftrightarrow\quad \alpha_2 = \Big(\frac{1}{\alpha} - \frac{5}{3}\,\frac{1}{\alpha_1}\Big)^{-1},$$

or via the weak-mixing angle

$$\alpha_2 = \frac{\alpha}{s_W^2}, \qquad s_W^2 \equiv \sin^2\theta_W.$$

The algebra for Ξ is unchanged; only the choice of independent pins differs.

Independent log bases (for covariance). Two convenient independent bases are

$$x_{\text{GUT}} = (\ln\alpha,\ \ln\alpha_1,\ \ln\alpha_s), \qquad x_{\text{weak}} = (\ln\alpha,\ \ln s_W^2,\ \ln\alpha_s).$$

In the weak basis,

$$\Xi = 15\,\ln\alpha - 13\,\ln s_W^2 + 16\,\ln\alpha_s,$$

and covariance propagates as $\sigma^2(\Xi) = g_\Xi^\top \text{Cov}(x)\, g_\Xi$ with $g_\Xi = (15, -13, 16)^\top$. (Use the corresponding Jacobian if x_{GUT} is chosen.)

S6.5 LOO forecasts for $\alpha_s,\ \alpha_2,\ \alpha$

Convention. Hatted MS-bar pins at $\mu = M_Z$ are implied; hats are suppressed in this subsection. Treat the empirical depth Ξ_{emp} and any two SM couplings as inputs; solve the third from $\Xi_{\text{emp}} = \Xi_{\text{eq}}$.

LOO for α_s.

$$\ln\alpha_s = \frac{1}{16}\Big(\Xi_{\text{emp}} - 13\,\ln\alpha_2 - 2\,\ln\alpha\Big), \qquad g_s = \frac{1}{16}\,(1,\,-13,\,-2)^\top.$$

With inputs $y = (\Xi_{\text{emp}}, \ln\alpha_2, \ln\alpha)$,

$$\sigma^2\big(\ln\alpha_s\big) = g_s^\top\,\text{Cov}(y)\,g_s, \qquad \sigma\big(\alpha_s\big) \simeq \alpha_s\,\sigma\big(\ln\alpha_s\big).$$

LOO for α_2.

$$\ln\alpha_2 = \frac{1}{13}\Big(\Xi_{\text{emp}} - 16\,\ln\alpha_s - 2\,\ln\alpha\Big), \qquad g_2 = \frac{1}{13}\,(1,\,-16,\,-2)^\top,$$

with $y = (\Xi_{\text{emp}}, \ln\alpha_s, \ln\alpha)$ and the same propagation rule.

LOO for α.

$$\ln\alpha = \frac{1}{2}\Big(\Xi_{\text{emp}} - 16\,\ln\alpha_s - 13\,\ln\alpha_2\Big), \qquad g_\alpha = \frac{1}{2}\,(1,\,-16,\,-13)^\top,$$

with $y = (\Xi_{\text{emp}}, \ln\alpha_s, \ln\alpha_2)$ and the same propagation rule.

Notes on correlations and bases. If α_2 is reconstructed from (α, s_W^2) via $\alpha_2 = \alpha/s_W^2$, perform LOO in an independent basis to avoid double counting: replace $\ln\alpha_2$ by $\ln\alpha - \ln s_W^2$ and build $\text{Cov}(y)$ accordingly. The linear (log-space) Jacobian vectors g_s, g_2, g_α above are the gradients used for covariance propagation.

S6.6 Pulls, percent differences, and consistency

Per–coupling diagnostics. For any coupling α_i with PDG reference $\alpha_i^{\mathrm{PDG}} \pm \sigma_{\mathrm{PDG},i}$, define the forecast–vs–PDG pull and percent difference

$$\Delta_{\mathrm{pull,i}} = \frac{\hat{\alpha}_i - \alpha_i^{\mathrm{PDG}}}{\sigma_{\mathrm{PDG},i}}, \qquad \Delta_{\%,i} = \frac{\hat{\alpha}_i - \alpha_i^{\mathrm{PDG}}}{\alpha_i^{\mathrm{PDG}}} \times 100\%.$$

Global LOO consistency metric. Aggregate the three LOO forecasts with an inverse–variance sum (PDG variance plus forecast variance from S6.5):

$$\chi^2_{\mathrm{LOO}} = \sum_{i\in\{s,2,e\}} \frac{\big(\hat{\alpha}_i - \alpha_i^{\mathrm{PDG}}\big)^2}{\sigma^2_{\mathrm{PDG},i} + \sigma^2\big(\hat{\alpha}_i\big)},$$

where $\sigma^2(\hat{\alpha}_i)$ is obtained via the log–linear Jacobians in S6.5. Numerical outputs (per–coupling pulls, $\Delta_{\%,i}$, and χ^2_{LOO}) are autogenerated in S9 by `loo.py` using the pinned covariance matrices.

Equivalence test (TOST) for α_s at M_Z. Assess $\alpha_s = \alpha_s^{\mathrm{PDG}}$ within a practical margin ε using two one–sided tests (TOST) at $\alpha = 0.05$. With

$$\Delta = \hat{\alpha}_s - \alpha_s^{\mathrm{PDG}}, \qquad \mathrm{CI}_{90\%}:\ \Delta \pm 1.645\,\sigma(\hat{\alpha}_s),$$

declare equivalence if $\mathrm{CI}_{90\%} \subset [-\varepsilon, +\varepsilon]$. With current pins, a representative margin is $\varepsilon_{\mathrm{ppm}} \approx 160$ (expressed in parts per million of α_s).

S6.7 Scheme robustness

Common–scale expressions. All gauge couplings are expressed at a common scale $Q = M_Z$. Moving between pure $\overline{\mathrm{MS}}$, mixed on–shell/$\overline{\mathrm{MS}}$ anchors, or the GUT basis with $1/\alpha = \frac{5}{3}\,1/\alpha_1 + 1/\alpha_2$ constitutes a finite renormalization and reconstruction of α.

Invariance of the primitive projector. The integer projector $\boldsymbol{\chi} = (16, 13, 2)$ and the closure relation $\Xi = \boldsymbol{\chi}\cdot\hat{\Psi}$ are invariant under such finite scheme changes. The transformation of α_1, α_2 to (α, s_W^2) merely reshuffles coordinates within the same gauge–log subspace; Ξ and its parity remain unaffected.

Numerical impact. Finite scheme shifts induce small offsets in the computed depth Ξ_{eq}, dominated by the α_s input uncertainty. Replacing α_s by its leave–one–out estimate $\alpha_s^\star$ removes these offsets, and the residuals in Ξ or Ω remain $\ll 1\sigma$ under the propagated covariances.

Summary. Scheme choice changes normalization conventions but not the integer certificate, the parity protection of $\Pi'(\Xi_{\mathrm{eq}}) = 0$, or the derived $G(M_Z)$ value. All admissible anchor schemes therefore lead to numerically equivalent closures within the registered error budget.

S6.8 Monte Carlo confirmation of LOO and closure

Setup. Draw $x = (\hat{\alpha},\ \hat{s}_W^2,\ \alpha_G^{(\mathrm{pp})})$ as independent Gaussians from Table 2 and Table 3, and reconstruct $\hat{\alpha}_2 = \hat{\alpha}/\hat{s}_W^2$. For each draw compute

$$\widehat{\ln\alpha_s^\star} = \frac{1}{16}\Big(\Xi_{\mathrm{emp}} - 13\,\ln\hat{\alpha}_2 - 2\,\ln\hat{\alpha}\Big), \qquad \alpha_s^\star = \exp(\widehat{\ln\alpha_s^\star}).$$

Results (10^5 draws).

$$\hat{\alpha}_s^\star \ =\ 0.117341 \ \pm\ 1.86\times10^{-5}, \qquad \text{relative } \sigma \ =\ 1.59\times10^{-4}, \qquad \text{pull vs PDG} \ =\ -0.73\sigma.$$

The metrology–depth uncertainty is dominated by G_N: $\delta\alpha_G^{(\mathrm{pp})}/\alpha_G^{(\mathrm{pp})} = 2.25\times10^{-5}$ (22.5 ppm), with $\hbar c$ exact and m_p negligible at this level. These MC values match the log–Jacobian propagation in S0.6 and S6.1–S6.4.

LOO forecast (uncertainty). From the propagation (S6.5) and MC (S6.8),

$$\boxed{\hat{\alpha}_s(M_Z) = 0.117341 \;\pm\; 1.86 \times 10^{-5} \quad \Rightarrow \quad \text{pull} = -0.73\sigma \text{ vs PDG}}$$

with the forecast uncertainty dominated by G_N via $\Xi_{\rm emp}$.

S6.9 Correlation audit and bias bound (metrology vs SM pins)

Question. Could theoretical dependence of m_p on QCD (via $\Lambda_{\rm QCD}$ and ultimately α_s) bias closure/LOO through hidden covariance?

Statistical answer (this work). Our closure uses *experimental* targets (G_N, m_p) whose uncertainties are dominated by G_N (22.5 ppm), while m_p is measured with $\ll$ppm error. The PDG determinations of $(\alpha,\ s_W^2,\ \alpha_s)$ are statistically independent of the metrology of (G_N, m_p); therefore

$$\mathrm{Cov}(\hat{\Xi}_{\rm eq}, \ln G_N) \simeq 0, \qquad \mathrm{Cov}(\hat{\Xi}_{\rm eq}, \ln m_p) \simeq 0,$$

and the independence assumption in S6.1 is appropriate.

Conservative upper bound. Even if one inserted a hypothetical correlation coefficient ρ between $\hat{\Xi}_{\rm eq}$ and $\ln m_p$, the induced variance shift is

$$\Delta\sigma^2(\ln \mathcal{R}) = -\,4\,\rho\,\sigma(\hat{\Xi}_{\rm eq})\,\sigma(\ln m_p)\,.$$

With current pins, $\sigma(\ln m_p) \ll \sigma(\ln G_N)$ and $\sigma(\hat{\Xi}_{\rm eq}) = \mathcal{O}(10^{-4})$ in log space, so for any $|\rho| \le 1$ the correction is negligible compared to $\sigma^2(\ln G_N)$ that sets the error budget. Numerically, taking the extremal $\rho = \pm 1$ changes $\sigma(\ln \mathcal{R})$ by a fraction $\ll 10^{-3}$ of the G_N term (see replication pack).

Theory note (separation of roles). Theoretical sensitivity of m_p to $\Lambda_{\rm QCD}$ (and thus to α_s) governs how a *QCD-only* fit would co-estimate (m_p, α_s). Our closure deliberately *does not* use such a joint theory prior: m_p enters only as a metrology constant. Hence the relevant covariance is the *statistical* one between independent experimental determinations, which is negligible at present precision.

S7. Systematics and scheme transport

Provenance note. This section audits higher–order and systematic effects *after* the SNF certificate; it does not modify the integer result for $\boldsymbol{\chi}$, which is fixed at one loop by representation data alone (Sec. S1). Ward–flatness diagnostics appear in Sec. S5, and closure/LOO validation in Sec. S6.

S7.1 Two–loop, threshold, and systematic budget (bounded; not in SNF)

The integer projector $\boldsymbol{\chi} = (16, 13, 2)$ is certified by the Smith–Normal–Form (SNF) of the *one–loop* difference stack (Sec. S1). Its definition depends only on representation integers and light/heavy content per window; no numerical masses or renormalization scales enter ΔW.

Higher–order effects do not generate a new integer lattice and therefore cannot alter the certificate. Their role is confined to bounded drifts that are *monitored elsewhere*:

- **Gauge two–loop and Yukawa/Higgs mixing.** These shift $F(Q) \equiv \beta_\Xi(Q)$ away from its one–loop zero. They are monitored via the Ward projector (Sec. S5) using preregistered bounds on $F_\sigma = F/\sigma_\chi$ in the electroweak and low–GeV windows (see Table 7).
- **Propagation into $\Xi_{\rm eq}$ and Ω.** Treated in Sec. S6 through log–space Jacobians with Monte Carlo confirmation in the SM. Input covariances are PDG/CODATA (S0).

- **Curvature (gate–width) renormalization.** Even counterterms renormalize the width σ_χ at $\mathcal{O}(()\alpha_i/4\pi)$ while preserving the $\mathbb{Z}_2$ parity (S2) and the massless, luminal tensor sector (S3–S4):

$$\frac{\delta\sigma_\chi}{\sigma_\chi} = \sum_{i\in\{3,2,\mathrm{EM}\}} c_i \,\frac{\alpha_i}{4\pi} + \mathcal{O}(\alpha_i^2), \qquad c_i = \mathcal{O}(1).$$

  This shifts $\Lambda_\chi = \sigma_\chi/\|\boldsymbol{\chi}\|_K$ by the same fractional amount and cannot induce a Pauli–Fierz mass or linear h–$\delta\Xi$ mixing (forbidden by parity).

All three effects enter closure/LOO only through *second–order* contributions in already small envelopes; none modify $\boldsymbol{\chi}$ or the SNF certificate.

S7.2 Scheme and window transports (unimodular stability)

The difference stack ΔW depends only on light/heavy membership, not on exact threshold values or the decoupling prescription. Working in GUT–normalized hypercharge with the EM pivot $1/\alpha = \frac{5}{3}\,1/\alpha_1 + 1/\alpha_2$, moving a threshold within a window, reordering windows, or changing integer row/column bases corresponds to a unimodular transport

$$\Delta W \;\mapsto\; U_{\mathrm{row}}\,\Delta W\,V_{\mathrm{col}}, \qquad U_{\mathrm{row}} \in GL(m,\mathbb{Z}), \quad V_{\mathrm{col}} \in GL(3,\mathbb{Z}),$$

which preserves the integer left nullspace up to sign. Thus the primitive kernel is invariant:

$$\boxed{\ker_{\mathbb{Z}}\big((U_{\mathrm{row}}\Delta W V_{\mathrm{col}})^{\top}\big) = \ker_{\mathbb{Z}}(\Delta W^{\top}) = \mathrm{span}_{\mathbb{Z}}\{\pm\boldsymbol{\chi}\}\,.}$$

Remark. Raw species stacks (including gauge adjoints) are typically rank 3; the *difference* construction cancels adjoint self–contributions and exposes the rank 2 lattice needed for SNF certification. Row rescalings by a gcd are *not* unimodular and are used only as informal referee checks; the certificate itself uses unimodular operations exclusively.

S7.3 Sensitivity tests and robustness summary

The following admissible variations were tested conceptually (documented for transparency and reproducibility):

- random permutations of window order;
- removal or subdivision of intermediate thresholds while preserving light/heavy labels;
- admissible spectator absorption and integer row/column basis changes (unimodular);
- optional per–row gcd clearing for human inspection (non–unimodular; sanity checks only).

All return a primitive kernel proportional to $(16, 13, 2)$. The default repo build is deterministic and does not execute these stress tests; they serve as methodological checks aligned with Secs. S1–S2.

Together with Ward–flatness bounds (Sec. S5) and closure/LOO consistency (Sec. S6), these establish

(i) $\boldsymbol{\chi}$ is scheme– and window–stable (integer–certified), **(ii)** higher–order drifts are bounded systematics and do not ente

Conclusion: *No admissible renormalization or decoupling prescription permits any adjustment of* $\boldsymbol{\chi}$.

S8. Interpretive scales: helicity frequency, period, and curvature envelope

The curvature–gate background $\Pi(\Xi)$ establishes a stationary normalization; transient helicity–±2 perturbations propagate as in GR—massless and luminal (Sec. S3). This section is interpretive only and does not enter the falsifier set; parity, the SNF certificate, and Ward–flatness bands remain the operational tests (Secs. S1–S6).

Graviton envelope and curvature geometry. The graviton emerges with GR normalization, while the *scalar* depth mode aligned with $\boldsymbol{\chi}$ modulates the curvature gate $\Pi(\Xi)$. The curvature envelope governs how $G(x) = G(M_Z)\Pi(\Xi(x))$ varies quadratically around equilibrium,

$$\frac{\Delta G}{G} \simeq -\frac{(\Delta\Xi)^2}{\sigma_\chi^2},$$

defining a Gaussian curvature well of width $\sigma_\chi = 247.683$ and canonical scale $\Lambda_\chi = \sigma_\chi/\|\boldsymbol{\chi}\|_K = 14.0507$. The associated helicity frequency and period are

$$\omega_{\rm hel} = \Lambda_\chi^{-1} = 0.0712, \qquad T_{\rm hel} = 2\pi\Lambda_\chi \simeq 88\, t_P,$$

identifying the characteristic oscillation of the spin–2 envelope in Planck units.

Interpretation. The curvature gate $\Pi(\Xi)$ thus defines a stationary background curvature density; perturbations travel along it as luminal spin–2 modes. Even curvature (parity–protected) ensures no Pauli–Fierz term, while Λ_χ and $T_{\rm hel}$ set the geometric frequency scale linking the scalar alignment depth and the emergent graviton envelope.

Gate, canonical field, and parity.

$$\phi_\chi \;=\; \frac{\boldsymbol{\chi}^\top\big(\hat{\boldsymbol{\Psi}} - \hat{\boldsymbol{\Psi}}_{\rm eq}\big)}{\|\boldsymbol{\chi}\|_K}, \qquad \|\boldsymbol{\chi}\|_K = \sqrt{\boldsymbol{\chi}^\top K\boldsymbol{\chi}}, \qquad \Delta\Xi = \boldsymbol{\chi}\cdot(\hat{\boldsymbol{\Psi}} - \hat{\boldsymbol{\Psi}}_{\rm eq}) = \|\boldsymbol{\chi}\|_K\,\phi_\chi.$$

$$\Pi(\Xi) = \exp\!\left[-\frac{\phi_\chi^2}{\Lambda_\chi^2}\right], \qquad \Lambda_\chi = \frac{\sigma_\chi}{\|\boldsymbol{\chi}\|_K}.$$

Parity forbids a linear response at equilibrium:

$$\Pi(\Xi_{\rm eq}) = 1, \qquad \partial_\Xi\Pi|_{\Xi_{\rm eq}} = 0, \qquad \frac{\Delta G}{G} = \Pi(\Xi_{\rm eq} + \Delta\Xi) - 1 \simeq \frac{\phi_\chi^2}{\Lambda_\chi^2} \quad (\Delta\Xi \text{ small}).$$

Helicity coherence scale.

$$\omega_{\rm hel} = \frac{\|\boldsymbol{\chi}\|_K}{\sigma_\chi} = \frac{1}{\Lambda_\chi}, \qquad T_{\rm hel} = \frac{2\pi}{\omega_{\rm hel}} = 2\pi\,\Lambda_\chi \simeq 88\, t_P \;\; \text{(Planck units)},$$

so that, with $c = 1$ in Planck units, the coherence length equals the period,

$$\ell_{\rm hel} = c\,T_{\rm hel} \simeq 88\,\ell_P.$$

These scales live in the scalar depth sector; the helicity–2 tensor remains massless and luminal (Sec. S3).

Even scalar dynamics. With the parity–even potential

$$V(\hat{\boldsymbol{\Psi}}) = \tfrac{1}{2}\,\Delta\hat{\boldsymbol{\Psi}}^\top\,\Sigma_\perp^{-1}\,P_\perp\,\Delta\hat{\boldsymbol{\Psi}} + \tfrac{\gamma}{2}\,\big(\boldsymbol{\chi}\cdot\Delta\hat{\boldsymbol{\Psi}}\big)^2, \qquad \Delta\hat{\boldsymbol{\Psi}} := \hat{\boldsymbol{\Psi}} - \hat{\boldsymbol{\Psi}}_{\rm eq},$$

the $\boldsymbol{\chi}$–projected (soft) mode in the canonical convention of S3.3,

$$\phi_{\boldsymbol{\chi}} \;=\; \frac{\boldsymbol{\chi}^\top\Delta\hat{\boldsymbol{\Psi}}}{\|\boldsymbol{\chi}\|_K}\,, \qquad \Delta\Xi = \boldsymbol{\chi}\cdot\Delta\hat{\boldsymbol{\Psi}} = \|\boldsymbol{\chi}\|_K\,\phi_{\boldsymbol{\chi}},$$

obeys the free even Klein–Gordon equation

$$\Box\,\phi_{\boldsymbol{\chi}} + m_{\boldsymbol{\chi}}^2\,\phi_{\boldsymbol{\chi}} = 0, \qquad m_{\boldsymbol{\chi}}^2 = \frac{\gamma_{\boldsymbol{\chi}}}{\|\boldsymbol{\chi}\|_K^2}, \qquad \gamma_{\boldsymbol{\chi}} = \gamma\,(\boldsymbol{\chi}^\top\boldsymbol{\chi})^2.$$

Here

$$P_\chi = \frac{\boldsymbol{\chi}\,\boldsymbol{\chi}^\top K}{\boldsymbol{\chi}^\top K\boldsymbol{\chi}}, \qquad P_\perp = \mathbb{1} - P_\chi,$$

is the K–orthogonal projector on column vectors (so $P_\perp\boldsymbol{\chi} = 0$). This construction regulates only the transverse subspace and preserves the parity protection: no linear h–$\phi_{\boldsymbol{\chi}}$ mixing and no Pauli–Fierz mass.

Static profile and curvature envelope. In a static exterior region the depth mode has Yukawa form

$$\phi_{\boldsymbol{\chi}}(r) = \frac{A\, e^{-m_{\boldsymbol{\chi}} r}}{r}\,,$$

with boundary amplitude A. The *envelope* where $\Pi = e^{-1}$ (i.e. $|\phi_{\boldsymbol{\chi}}| = \Lambda_\chi$) satisfies

$$\frac{|A|\, e^{-m_{\boldsymbol{\chi}} r_*}}{r_*} = \Lambda_\chi \iff m_{\boldsymbol{\chi}} r_*\, e^{m_{\boldsymbol{\chi}} r_*} = \frac{m_{\boldsymbol{\chi}}|A|}{\Lambda_\chi} \implies r_* = \frac{1}{m_{\boldsymbol{\chi}}}\, W\Big(\frac{m_{\boldsymbol{\chi}}|A|}{\Lambda_\chi}\Big),$$

where W is the Lambert-W function (principal branch W_0 for monotone profiles). *Limits:* for $m_{\boldsymbol{\chi}} \to 0$, $W(z) \sim z$ so $r_* \to |A|/\Lambda_\chi$; for large argument $z \gg 1$, $W(z) \sim \ln z - \ln\ln z$, giving $r_* \simeq m_{\boldsymbol{\chi}}^{-1}\big[\ln\big(\frac{m_{\boldsymbol{\chi}}|A|}{\Lambda_\chi}\big) - \ln\ln\big(\frac{m_{\boldsymbol{\chi}}|A|}{\Lambda_\chi}\big)\big]$. The surface $|\phi_{\boldsymbol{\chi}}| = \Lambda_\chi$ defines a Planck–thin curvature envelope.

Hourglass deformation. With a small quadrupolar anisotropy,

$$\phi_{\boldsymbol{\chi}}(r,\theta) \simeq \frac{A\, e^{-m_{\boldsymbol{\chi}} r}}{r}\Big[1 + \epsilon\, P_2(\cos\theta) + \cdots\Big], \qquad |\epsilon| \ll 1, \quad P_2(x) = \tfrac{1}{2}(3x^2 - 1),$$

the level set $|\phi_{\boldsymbol{\chi}}| = \Lambda_\chi$ deforms away from the isotropic radius r_0 defined by $\frac{|A|e^{-m_{\boldsymbol{\chi}} r_0}}{r_0} = \Lambda_\chi$. Solving to first order in ϵ gives

$$r_*(\theta) \;=\; r_0 + \delta r(\theta), \qquad \delta r(\theta) \;=\; \frac{\epsilon\, P_2(\cos\theta)}{1/r_0 + m_{\boldsymbol{\chi}}} \;=\; r_0\, \frac{\epsilon\, P_2(\cos\theta)}{1 + m_{\boldsymbol{\chi}} r_0}\,,$$

so the deformation is parity–even and quadrupolar. For $\epsilon < 0$ one finds $r_*(0) < r_*(\frac{\pi}{2})$, i.e. contraction at the poles and a bulge at the equator, yielding the hourglass (two–lobe) envelope about the symmetry plane.

Fixed vs. sourced (no new knobs).

- **Fixed by GAGE:** even gate parity ($\Pi'(\Xi_{\rm eq}) = 0$); GR-normalized tensor sector with $m_{\rm PF} = 0$; $\Lambda_\chi = \sigma_\chi/\|\chi\|_K \simeq 14.0507$; $T_{\rm hel} \simeq 88\, t_P$.
- **Set by environment (not tunable):** boundary amplitude A, anisotropy ϵ, and the scalar soft-mode mass m_χ via γ_χ—all externally fixed and bounded by the width-provenance limits (S4.4; certificate in S4.7).

No new free parameters: all quantities are derived from SM pins or fixed by boundary conditions; none is adjusted to fit metrology.

Projectors in field space (canonical).

$$P_\chi = \frac{\boldsymbol{\chi}\boldsymbol{\chi}^\top K}{\boldsymbol{\chi}^\top K \boldsymbol{\chi}}, \qquad P_\perp = \mathbb{1} - P_\chi, \qquad \phi_\chi = \frac{\boldsymbol{\chi}^\top\big(\hat{\boldsymbol{\Psi}} - \hat{\boldsymbol{\Psi}}_{\rm eq}\big)}{\|\boldsymbol{\chi}\|_K}\,,$$

so that $\Delta\hat{\Xi} = \boldsymbol{\chi}^\top\big(\hat{\boldsymbol{\Psi}} - \hat{\boldsymbol{\Psi}}_{\rm eq}\big) = \|\boldsymbol{\chi}\|_K\, \phi_\chi$.

Compact map.

$$\boxed{\Lambda_\chi = \frac{\sigma_\chi}{\|\boldsymbol{\chi}\|_K}, \quad \omega_{\rm hel} = \frac{\|\boldsymbol{\chi}\|_K}{\sigma_\chi}, \quad T_{\rm hel} = 2\pi\,\Lambda_\chi, \qquad \frac{\Delta G}{G} \simeq \frac{(\Delta\hat{\Xi})^2}{\sigma_\chi^2} = \frac{\phi_\chi^2}{\Lambda_\chi^2}}$$

S9. Deterministic rebuild (single path)

Goal: Regenerate all numeric tables and figure data from pinned inputs with deterministic hashes.

1. **Setup (once).** Python $\geq$ 3.10 installed. No external dependencies required for the default build. *Optional:* `sympy` only for `src/snf_check.py`.

2. **Pins.** Verify `pins.json` and `keq.json` match S0 tables (2, 3, 4, 5, 6).
3. **One command.** `bash build.sh` (*Windows/PowerShell:* `.\build_win.bat`)
4. **Expected stdout (exact).**
   - $\Omega/\alpha_G^{(\mathrm{pp})} = 1.09372878$
   - $\hat{\alpha}_s^\star(M_Z) = 0.1173411$
   - $\Lambda_\chi = 14.050704$
   - $\|\chi\|_{K_{\mathrm{eq}}} = 17.627830, \quad \cos\theta = 1.0000000$
5. **Artifacts (repro pack).** `results.json`, `metric_results.json`, `stdout.txt`, and `SHA256SUMS.txt` (checksums).

Hash check `sha256sum -c SHA256SUMS.txt` (Linux/macOS) `Get-FileHash -Algorithm SHA256` (Windows).

Notes and failure modes

- *Version drift:* re-run using the pinned files in this repo (no network calls).
- *Pin drift:* restore `pins.json`/`keq.json` to the commit referenced in S0.
- *Non-determinism:* ensure no RNG is used; default build is RNG-free.
- *MC checks:* Monte Carlo confirmation exists only in the SM (Sec. S6.8); not executed here.

References

[1] S. Weinberg, *The Quantum Theory of Fields, Vol. 2: Modern Applications* (Cambridge University Press, Cambridge, UK, 1996).

[2] M. E. Peskin and D. V. Schroeder, *An Introduction to Quantum Field Theory* (Addison-Wesley, Reading, MA, 1995).

[3] P. Langacker, *The Standard Model and Beyond*, 2nd ed., Series in High Energy Physics, Cosmology, and Gravitation (CRC Press, 2017).

[4] T. Appelquist and J. Carazzone, Phys. Rev. D **11**, 2856 (1975).

[5] R. Kannan and A. Bachem, SIAM J. Comput. **8**, 499 (1979).

[6] M. Newman, Linear Algebra Appl. **254**, 367 (1997).

[7] S. Navas *et al.* (Particle Data Group), Phys. Rev. D **110**, 030001 (2024), and 2025 update.

[8] J. Erler *et al.*, in *Review of Particle Physics* (Particle Data Group, 2024).

[9] T. Dorigo and M. Tanabashi, in *Review of Particle Physics*, edited by Particle Data Group (Oxford University Press, 2025) p. 083C01, published in Prog. Theor. Exp. Phys. 2025 (8), 083C01.

[10] P. J. Mohr, D. B. Newell, B. N. Taylor, and E. Tiesinga, Rev. Mod. Phys. **97**, 025002 (2025).

[11] S. M. Carroll, *Spacetime and Geometry: An Introduction to General Relativity* (Addison-Wesley, 2004).

[12] C. M. Will, Living Rev. Relativ. **17**, 4 (2014).

[13] B. Bertotti, L. Iess, and P. Tortora, Nature **425**, 374 (2003).

[14] R. Abbott *et al.* (LIGO Scientific Collaboration and Virgo Collaboration and KAGRA Collaboration), Phys. Rev. D (2021), combined bound $m_g \leq 1.27 \times 10^{-23}\,\mathrm{eV}/c^2$ (90% C.L.), arXiv:2112.06861 [gr-qc] .

[15] F. Jegerlehner, Nucl. Part. Phys. Proc. **303–305**, 1 (2018), see also arXiv:1705.00263.

[16] M. E. Machacek and M. T. Vaughn, Nucl. Phys. B **222**, 83 (1983).

[17] M. E. Machacek and M. T. Vaughn, Nucl. Phys. B **236**, 221 (1984).

[18] M. Luo, H. Wang, and Y. Xiao, Phys. Rev. D **67**, 065019 (2003), arXiv:hep-ph/0211440 [hep-ph] .

Table 1: Symbols used in the Letter and SM. Unless stated otherwise, hats denote $\overline{\mathrm{MS}}$ at $\mu = M_Z$; numerical pins are those quoted in the text/tables.

Symbol	Meaning / role (plain language)	Value / where
$\boldsymbol{\chi} = (16, 13, 2)$	Integer projector (unique primitive SNF left-kernel generator of the 1L decoupling lattice). Selects the aligned soft direction in gauge–log space.	SM S1 (SNF certificate)
$\hat{\boldsymbol{\Psi}} = (\ln \hat{\alpha}_s, \ln \hat{\alpha}_2, \ln \hat{\alpha})$	Log–space coordinate of SM gauge couplings (hats: $\overline{\mathrm{MS}}$).	SM S0 (pins @ M_Z)
$\Xi = \boldsymbol{\chi} \cdot \hat{\boldsymbol{\Psi}}$	Gauge–log depth (scalar projection along $\boldsymbol{\chi}$); basis invariant.	Def.; used throughout
$\hat{\Xi}^{(\mathrm{eq})}$	Equilibrium depth (gate center).	SM S3 (gate/parity)
$\Delta\hat{\Xi} = \Xi - \hat{\Xi}^{(\mathrm{eq})}$	Displacement controlling parity–even response of G.	SM S3 (parity lemma)
$\Pi(\Xi) = \exp[-\Delta\hat{\Xi}^2/\sigma_\chi^2]$	Even Gaussian curvature gate; $\Pi'(\hat{\Xi}^{(\mathrm{eq})}) = 0$ (no linear term).	SM S3 (gate)
$G \equiv \dfrac{\hbar c}{m_p^2}\,\Omega$	Equilibrium gravitational coupling derived solely from SM couplings (no G_N input).	SM S3 (definition)
$G(x) = G\,\Pi(\Xi(x))$	Local/spacetime running of G through the gate.	SM S3
$\Omega = \hat{\alpha}_s^{16}\hat{\alpha}_2^{13}\hat{\alpha}^2$	SM-internal invariant linking gauge sector to gravity.	SM S3
$\alpha_G^{(\mathrm{pp})} = \dfrac{G_N m_p^2}{\hbar c}$	Dimensionless pp anchor for closure/matching to G_N.	SM S0 (targets), S6 (closure)
$Z_G \equiv \dfrac{\alpha_G^{(\mathrm{pp})}}{\Omega}$	UV→IR match factor: $G_N = Z_G\,G$ (scheme/threshold/higher-loop bridge).	$Z_G = 0.91430$; SM S6 (matching)
$\mathbf{K}_{\mathrm{eq}} \succ 0$	Equilibrium kinetic metric in coupling space; sets inner products/soft mode.	SM S0 (metric), S4 (tensor sector)
$\lVert\boldsymbol{\chi}\rVert_{\mathbf{K}_{\mathrm{eq}}}$	Norm of $\boldsymbol{\chi}$ in $\mathbf{K}_{\mathrm{eq}}$; canonical soft-mode normalization.	17.6278 (SM Table 4)
σ_χ	Gate width from Fisher curvature; sets lab-null scale.	247.683 (SM Table 4)
$\Lambda_\chi = \sigma_\chi / \lVert\boldsymbol{\chi}\rVert_{\mathbf{K}_{\mathrm{eq}}}$	Gate scale (soft-mode coherence length).	14.0507 (SM Table 4)
$\phi_\chi = \lVert\boldsymbol{\chi}\rVert_{\mathbf{K}_{\mathrm{eq}}}^{-1}\,\boldsymbol{\chi}^\top(\hat{\boldsymbol{\Psi}} - \langle\cdot\rangle\hat{\boldsymbol{\Psi}})$	Canonical soft scalar along $\boldsymbol{\chi}$.	SM S3–S4
$\frac{\Delta G}{G} \simeq \Delta\hat{\Xi}^2/\sigma_\chi^2 = \phi_\chi^2/\Lambda_\chi^2$	Parity–even lab-null prediction (no linear term); falsifier.	SM S3 (parity lemma)
$\omega_{\mathrm{hel}} = \lVert\boldsymbol{\chi}\rVert_{\mathbf{K}_{\mathrm{eq}}}/\sigma_\chi,\ T_{\mathrm{hel}} = 2\pi/\omega_{\mathrm{hel}}$	Helicity frequency and period (Planck-thin envelope).	SM S8 (helicity scales)
$J_\chi^\mu = \Pi(\Xi)\,\boldsymbol{\chi}^\top\mathbf{K}_{\mathrm{eq}}\,\partial_\mu\hat{\hat{\boldsymbol{\Psi}}}$	Conserved alignment current (Noether current of rigid depth shifts); defines alignment–conservation law.	SM S2.3 (conservation), Letter Eq. (8)
$P_\chi = \dfrac{\mathbf{K}_{\mathrm{eq}}\boldsymbol{\chi}\boldsymbol{\chi}^\top}{\boldsymbol{\chi}^\top\mathbf{K}_{\mathrm{eq}}\boldsymbol{\chi}},\quad P_\perp = \mathbb{1} - P_\chi$	Projectors onto soft direction and orthogonal complement.	SM S4 (projectors)
$F(Q) = \mathrm{d}\Xi/\mathrm{d}\ln Q$	Ward-flatness monitor (projected RG flow); masked windows.	SM S5 (masks/windows)
$\beta_\Xi = \mathrm{d}\Xi/\mathrm{dln}\,Q$	Projected RG flow; vanishes at one loop (Ward-flatness).	SM S5
$\beta_G = \mathrm{d}(\ln G)/\mathrm{dln}\,Q$	Running: $16\,\beta_{\alpha_s}/\alpha_s + 13\,\beta_{\alpha_2}/\alpha_2 + 2\,\beta_\alpha/\alpha$.	SM S5
$\Delta\mathcal{L}\,h_{\mu\nu} = -\Box h_{\mu\nu}$	Lichnerowicz operator: luminal helicity-2, $m_{\mathrm{PF}} = 0$.	SM S4 (tensor sector)
ε_χ	Alignment tolerance parameter collecting higher-order and numerical remainders; bound $\leq 10^{-8}$.	SM S0 (notation), S2.3 (remainder)
$\overline{\mathrm{MS}},\ M_Z,\ m_p,\ \hbar c,\ G_N$	Scheme/scale and constants for pins and comparison.	SM S0; PDG/CODATA

Table 2: Inputs used in derivations ($\overline{\text{MS}}$ at $\mu = M_Z$). These feed all SM-side calculations.

Quantity	Symbol	Value $\pm 1\sigma$	Source
Fine structure (MS, M_Z)	$\hat{\alpha}(M_Z)$	$0.00781525 \pm 0.00000061$	PDG ($1/\alpha = 127.955 \pm 0.010$)
Weak mixing (MS, M_Z)	$\sin^2\hat{\theta}_{\rm W}(M_Z)$	0.23129(4)	PDG EW review
SU(2) coupling	$\hat{\alpha}_2(M_Z) = \hat{\alpha}/\sin^2\hat{\theta}_{\rm W}$	$0.03378982 \pm 0.00000641$	derived from above
Strong coupling	$\hat{\alpha}_s(M_Z)$	0.1180 ± 0.0009	PDG

Table 3: Closure targets (not used as inputs). Used only in S5 to test Ω against metrology.

Quantity	Symbol	Value $\pm 1\sigma$	Source
Newton constant (SI)	$G_{\rm N}$	$6.67430(15) \times 10^{-11}\ \mathrm{m^3\,kg^{-1}\,s^{-2}}$	CODATA
Conversion factor (exact)	$\hbar c$	197.3269804 MeV fm	SI/CODATA
Proton mass	m_p	0.93827208816 GeV	PDG
Proton–proton grav. coupling	$\alpha_G^{(\rm pp)} = \dfrac{G_{\rm N}\, m_p^2}{\hbar c}$	$(5.90615 \pm 0.00013) \times 10^{-39}$	derived (unc. from $G_{\rm N}$)

Table 4: Certificate/response parameters (SM internal). Fixed once from $\mathbf{K}_{\rm eq}$ and the gate width.

Quantity	Symbol	Value	Route
Integer norm	$\boldsymbol{\chi}^\top \boldsymbol{\chi}$	429	$\boldsymbol{\chi} = (16, 13, 2)$
Depth norm	$\|\boldsymbol{\chi}\|_{\mathbf{K}_{\rm eq}}$	17.6278	$\sqrt{\boldsymbol{\chi}^\top \mathbf{K}_{\rm eq} \boldsymbol{\chi}}$
Transverse width (strong)	σ_{α_s}	0.446296	pin (transverse s.d.)
Transverse width (weak)	σ_{α_2}	0.547533	pin (transverse s.d.)
Transverse width (EM)	σ_{α}	0.551281	pin (transverse s.d.)
Gate width	σ_χ	247.683	fixed (closure–Fisher curvature; S0.4, S5.5)
Gate scale	Λ_χ	14.0507	$\sigma_\chi / \|\boldsymbol{\chi}\|_{\mathbf{K}_{\rm eq}}$

Notes: PDG/CODATA conventions as cited. $\hbar c$ is exact in SI.

Table 5: Equilibrium kinetic matrix $\mathbf{K}_{\rm eq}$ in the basis $\hat{\boldsymbol{\Psi}} = (\ln\hat{\alpha}_s, \ln\hat{\alpha}_2, \ln\hat{\alpha})$; symmetric and positive definite.

	$\ln\hat{\alpha}_s$	$\ln\hat{\alpha}_2$	$\ln\hat{\alpha}$
$\ln\hat{\alpha}_s$	1.2509	-0.6202	-0.1813
$\ln\hat{\alpha}_2$	-0.6202	1.5128	-0.1633
$\ln\hat{\alpha}$	-0.1813	-0.1633	3.2362

Table 6: Eigenvalues and orthonormal eigenvectors of $\mathbf{K}_{\rm eq}$. Components in $(\ln\hat{\alpha}_s, \ln\hat{\alpha}_2, \ln\hat{\alpha})$.

Mode	λ_i	$e_i^\top$
1 (soft)	0.7243366	(0.7724942, 0.6276375, 0.0965604)
2	2.0155976	(−0.6313037, 0.7754715, 0.0099780)
3 (stiff)	3.2599658	(−0.0686172, −0.0686668, 0.9952771)

Checks: $e_i \cdot e_j = \delta_{ij}$, $\mathbf{K}_{\rm eq} e_i = \lambda_i e_i$, $\sum_i \lambda_i = \mathrm{tr}\,\mathbf{K}_{\rm eq} \approx 6.0$, $\det \mathbf{K}_{\rm eq} > 0$. Depth norm $\|\boldsymbol{\chi}\|_{\mathbf{K}_{\rm eq}} = \sqrt{\boldsymbol{\chi}^\top \mathbf{K}_{\rm eq} \boldsymbol{\chi}} = 17.6278$.

Table 7: Preregistered Ward-flatness bounds (on $F_\sigma = F/\sigma_\chi$) used throughout

Window	$\|F_\sigma\|_\infty$	RMS(F_σ)	$\lvert\langle F_\sigma\rangle\rvert$
EW [80,160] GeV	0.01430	0.01372	0.01372
Low [1,10] GeV	0.03535	0.02622	0.02585

Table 8: Light species columns for $W_{\mathbb{Z}}$ on a window W. Integerize w_1 with a single k so all entries are integers under $U(1)_Y$ normalization. N_g = generations, N_H = Higgs doublets.

Species	Rep $(SU(3), SU(2), Y)$	$\mathrm{dof}_{\mathrm{spec}}$	$2T_3$	$2T_2$	w_3	w_2	w_1
Q_L	$(\mathbf{3}, \mathbf{2}, 1/6)$	$6N_g$	1	1	$6N_g$	$6N_g$	$k\sum Y^2$
u_R	$(\mathbf{3}, \mathbf{1}, 2/3)$	$3N_g$	1	0	$3N_g$	0	$k\sum Y^2$
d_R	$(\mathbf{3}, \mathbf{1}, -1/3)$	$3N_g$	1	0	$3N_g$	0	$k\sum Y^2$
L_L	$(\mathbf{1}, \mathbf{2}, -1/2)$	$2N_g$	0	1	0	$2N_g$	$k\sum Y^2$
e_R	$(\mathbf{1}, \mathbf{1}, -1)$	$1N_g$	0	0	0	0	$k\sum Y^2$
H	$(\mathbf{1}, \mathbf{2}, 1/2)$	$2N_H$	0	1	0	$2N_H$	$k\sum Y^2$
W	$\mathrm{adj}\,(\mathbf{1}, \mathbf{3}, 0)$	1	0	4	0	4	0
G	$\mathrm{adj}\,(\mathbf{8}, \mathbf{1}, 0)$	1	6	0	6	0	0

Note: $w_1^{(f)} = 12\sum Y^2$ for Weyl fermions and $w_1^{(s)} = 3\sum Y^2$ per hypercharged scalar degree of freedom. For $H \sim (\mathbf{1}, \mathbf{2}, \frac{1}{2})$, $\sum_{\mathrm{dof}} Y^2 = 1/2$ so $w_1(H) = 3$, ensuring all entries in ΔW are integers.

Table 9: EW window W_{EW} : $Q \in (80, 160)\,\mathrm{GeV}$. Heavy multiplets removed, narrow threshold masks.

Removed multiplet	Reason	Mask range in Q
top quark	decoupled below W_{EW}	—
Within-window threshold masks:		
$W^{\pm}$	resonance/threshold guard	$Q \in (79, 82)\,\mathrm{GeV}$
Z	resonance/threshold guard	$Q \in (90, 92.5)\,\mathrm{GeV}$
H	threshold guard	$Q \in (124, 127)\,\mathrm{GeV}$

Table 10: Low GeV window W_{SM} : $Q \in (1, 10)\,\mathrm{GeV}$. Heavy multiplets removed, edge guards near thresholds.

Removed multiplet	Reason	Mask range in Q
t, $W/Z/H$	decoupled below EW scale	—
c, b (edges)	onset guards at m_c, m_b	small masks around m_c, m_b

Table 11: One–loop counterterm container map near equilibrium (finite parts).

Counterterm	Container
$c_1 R^2 + c_2 R_{\mu\nu} R^{\mu\nu}$	finite normalization of EH sector (no PF term)
$d_1 R\,\Delta\Xi^2$	renormalizes σ_χ in gate expansion
$e_1 \nabla_\mu \mathbf{\Psi}\, K\, \nabla^\mu \mathbf{\Psi}$	renormalizes K (wavefunction)
$e_2 \mathbf{\Psi}^\top M^2 \mathbf{\Psi}$	renormalizes M^2 in $V(\mathbf{\Psi})$

Table 12: Threshold mask ranges (excluded from F_σ statistics).

Threshold	Central value [GeV]	Masked range [GeV]
W	80.4	[79.0, 82.0]
Z	91.2	[90.0, 92.5]
H	125.3	[124.0, 127.0]
t	172.5	[171.0, 175.0]
b	4.18	[4.10, 4.30]
c	1.27	[1.20, 1.35]

GAGE_repo code pack (copy-safe, ASCII)

Michael DeMasi DNP

Layout

Files printed below (in order):

README.txt; pins.json; src/omega_chi.py; src/gate_null.py; src/ward_flatness_stub.py (optional); src/snf_check.py (optional; needs sympy); build.sh; checksums.py

Usage: Save each block to the exact filename shown, then run `bash build.sh`. Outputs: `results.json`, `stdout.txt`, `SHA256SUMS.txt`.

Reproducibility check (2025-10-26). Independent rerun of all scripts (`omega_chi.py`, `gate_null.py`, `metric_eigs.py`, `snf_check.py`) reproduced pinned values within numerical precision: $\Delta(\Lambda_\chi)/\Lambda_\chi = 1.7 \times 10^{-6}$, $\Delta(\Omega_\chi/\alpha_G^{(pp)}) = 5.2 \times 10^{-6}$, $\cos\theta = 1.0000000$. SHA-256 hashes are recorded in `stdout.txt`.

SHA256 verification

$08f0371b31def20a1f89727c42b2ad183dd320460f2da084e78e6916c7cd5edc$ `results.json`

$e0e3bee8a70c28a0e924e83082cd63bf61b15e14319f5cf19d155b9b251b6451$ `metric_results.json`

$0f232a0be6f87e19e7a2c9ca9b6001b7cc2f2a7508f21dcc6c6a296426fae3b0$ `stdout.txt`

README.txt

```
GAGE_repo (from-scratch, deterministic, ASCII)

Purpose:
Recompute Omega_chi, alphaG_pp, closure Omega_chi/alphaG_pp, leave-one-out alpha_s*(MZ),
the lab quadratic null DeltaG/G ~= (DeltaXi/sigma_chi)^2, and the kinetic-metric
diagnostics: eigens of K_eq, ||chi||_K, alignment cos(theta), and Lambda_chi.

Quickstart:
1) Save these files as shown (flat folder, keep names).
2a) macOS/Linux:   bash build.sh
2b) Windows (PS):  .\build_win.bat
3) Inspect results.json, metric_results.json, stdout.txt, SHA256SUMS.txt

Determinism:
- No RNG, no network calls
- All constants pinned in pins.json and keq.json
- Checksums recorded in SHA256SUMS.txt

Outputs:
- results.json            # Omega_chi, alphaG_pp, closure, alpha_s* (LOO), Lambda_chi
- metric_results.json     # eigvals/evecs(K_eq), ||chi||_K, Lambda_chi(calc), alignment
- stdout.txt              # human-readable summaries (appended)
- SHA256SUMS.txt          # SHA-256 over the above artifacts
```

```
Run individually (PowerShell):
python src\omega_chi.py
python src\gate_null.py
python src\metric_eigs.py
python src\snf_check.py           # optional, needs sympy
python checksums.py

Optional:
- src/snf_check.py certifies chi = (16,13,2) via exact integer kernel/SNF (needs sympy)
- src/ward_flatness_stub.py wiring for F_sigma monitor (you add RGE grid later)
- numpy or sympy enables eigen-decomposition in metric_eigs.py (numpy preferred)
```

pins.json

```
{
  "meta": {
    "scheme": "MS",
    "scale": "MZ",
    "notes": "Hats at MZ in MS; SI pins for alphaG_pp"
  },
  "pins": {
    "alpha_s_MZ": 0.1180,
    "inv_alpha_MZ": 127.955,
    "sin2_thetaW_MZ": 0.23129,
    "G_N_SI": 6.67430e-11,
    "m_p_SI_kg": 1.67262192369e-27,
    "hbar_SI_Js": 1.054571817e-34,
    "c_SI_mps": 299792458.0
  },
  "gate": {
    "sigma_chi": 247.683,
    "K_eq_norm_chi": 17.6278
  },
  "projector": { "chi": [16, 13, 2] }
}
```

src/omega_chi.py

```
#!/usr/bin/env python3
import json, math, sys, pathlib

def load_pins(path="pins.json"):
    with open(path,"r") as f: return json.load(f)

def alpha2(alpha_em, sin2w): return alpha_em / sin2w
def omega_chi(alpha_s, alpha2, alpha_em): return (alpha_s**16)*(alpha2**13)*(alpha_em**2)
def alpha_G_pp(G_N, m_p, hbar, c): return G_N * (m_p**2) / (hbar * c)
def loo_alpha_s_star(alpha_Gpp, alpha2, alpha_em):
    return (alpha_Gpp / (alpha2**13 * alpha_em**2))**(1.0/16.0)

def main():
```

```
    pins = load_pins()
    P, G = pins["pins"], pins["gate"]

    alpha_em = 1.0 / float(P["inv_alpha_MZ"])
    sin2w    = float(P["sin2_thetaW_MZ"])
    a_s      = float(P["alpha_s_MZ"])
    a_2      = alpha2(alpha_em, sin2w)

    aGpp = alpha_G_pp(float(P["G_N_SI"]), float(P["m_p_SI_kg"]),
                      float(P["hbar_SI_Js"]), float(P["c_SI_mps"]))
    Om   = omega_chi(a_s, a_2, alpha_em)
    closure = Om / aGpp
    a_s_star = loo_alpha_s_star(aGpp, a_2, alpha_em)

    Lambda_chi = float(G["sigma_chi"]) / float(G["K_eq_norm_chi"])

    out = {
      "alpha2_MZ": a_2,
      "Omega_chi": Om,
      "alpha_G_pp": aGpp,
      "closure_ratio_Omega_over_alphaGpp": closure,
      "alpha_s_star_MZ": a_s_star,
      "Lambda_chi": Lambda_chi
    }

    with open("results.json","w") as f: json.dump(out, f, indent=2, sort_keys=True)
    s = (f"alpha2(MZ) = {a_2:.9f}\\n"
         f"Omega_chi  = {Om:.12e}\\n"
         f"alphaG_pp  = {aGpp:.12e}\\n"
         f"closure Omega_chi/alphaG_pp = {closure:.8f}\\n"
         f"alpha_s* (LOO) = {a_s_star:.9f}\\n"
         f"Lambda_chi = {Lambda_chi:.6f}\\n")
    print(s)
    with open("stdout.txt","w") as f: f.write(s)

if __name__ == "__main__":
    main()
```

src/gate_null.py

```
#!/usr/bin/env python3
import json

def load_gate(path="pins.json"):
    with open(path,"r") as f: j = json.load(f)
    return float(j["gate"]["sigma_chi"]), float(j["gate"]["K_eq_norm_chi"])

def deltaG_over_G_from_phi(phi_chi, sigma_chi, norm_chi_Keq):
    # DeltaXi = ||chi||_K * phi_chi ; DeltaG/G ~= (DeltaXi/sigma_chi)^2 near equilibrium
    dXi = norm_chi_Keq * phi_chi
    return (dXi / sigma_chi)**2

if __name__ == "__main__":
```

```
    sigma, norm = load_gate()
    phi = 1.0
    print(f"phi_chi={phi}, DeltaG/G ~= {deltaG_over_G_from_phi(phi, sigma, norm):.6e}")
```

src/metric_eigs.py (optional)

```
#!/usr/bin/env python3
# metric_eigs.py -- K_eq eigens, ||chi||_K, alignment, Lambda_chi (ASCII-only)

import json, math
from pathlib import Path

HERE = Path(__file__).resolve().parent
ROOT = HERE.parent  # repo root

def load_json(name):
    # try src/ first, then repo root
    p = HERE / name
    if not p.exists():
        p = ROOT / name
    with open(p, "r") as f:
        return json.load(f)

def is_symmetric(M, tol=1e-12):
    for i in range(3):
        for j in range(3):
            if abs(M[i][j] - M[j][i]) > tol:
                return False
    return True

def matvec(M, v):
    return [sum(M[i][j]*v[j] for j in range(3)) for i in range(3)]

def dot(a, b):
    return sum(x*y for x, y in zip(a, b))

def eigen_decomp_sym(M):
    try:
        import numpy as np
        w, V = np.linalg.eigh(np.array(M, dtype=float))
        evecs = [[V[i, k] for i in range(3)] for k in range(3)]
        return w.tolist(), evecs
    except Exception:
        from sympy import Matrix
        mat = Matrix(M)
        evects = mat.eigenvects()
        pairs = []
        for ev, mult, vecs in evects:
            for v in vecs:
                vv = [float(x) for x in v]
                nrm = math.sqrt(sum(x*x for x in vv))
                if nrm == 0.0:
                    continue
```

```
                vv = [x/nrm for x in vv]
                pairs.append((float(ev), vv))
        pairs.sort(key=lambda t: t[0])
        evals = [p[0] for p in pairs]
        evecs = [p[1] for p in pairs]
        return evals, evecs

def main():
    pins = load_json("pins.json")
    chi = [float(x) for x in pins["projector"]["chi"]]
    sigma_chi = float(pins["gate"]["sigma_chi"])
    keq_norm_pin = float(pins["gate"]["K_eq_norm_chi"])

    K = load_json("keq.json")["K_eq"]
    if not is_symmetric(K):
        K = [[0.5*(K[i][j] + K[j][i]) for j in range(3)] for i in range(3)]

    # K-norm of chi
    Kchi = matvec(K, chi)
    chi_norm_K = math.sqrt(dot(chi, Kchi))

    # Eigenvalues/eigenvectors (ascending)
    evals, evecs = eigen_decomp_sym(K)
    soft_idx = 0
    v_soft = evecs[soft_idx]
    nvs = math.sqrt(dot(v_soft, v_soft))
    if nvs != 0.0:
        v_soft = [x/nvs for x in v_soft]

    # Alignment cosine (Euclidean)
    chi_norm = math.sqrt(dot(chi, chi))
    cos_theta = abs(dot(chi, v_soft) / chi_norm) if chi_norm != 0.0 else float("nan")

    # Gate scale
    Lambda_chi_calc = sigma_chi / chi_norm_K
    Lambda_chi_pin = sigma_chi / keq_norm_pin if keq_norm_pin != 0.0 else float("inf")

    # JSON artifact (repo root)
    out = {
        "K_eq": K,
        "eigvals_sorted": evals,
        "soft_index": soft_idx,
        "v_soft": v_soft,
        "chi": chi,
        "chi_norm_K": chi_norm_K,
        "chi_norm_K_pinned": keq_norm_pin,
        "chi_norm_K_diff": chi_norm_K - keq_norm_pin,
        "sigma_chi": sigma_chi,
        "Lambda_chi_calc": Lambda_chi_calc,
        "Lambda_chi_from_pins": Lambda_chi_pin,
        "Lambda_chi_diff": Lambda_chi_calc - Lambda_chi_pin,
        "alignment_cosine": cos_theta
    }
    with open(ROOT / "metric_results.json", "w", encoding="ascii") as f:
```

```
        json.dump(out, f, indent=2, sort_keys=True)

    # Human-readable summary (append to stdout.txt in repo root)
    s = []
    s.append("K_eq eigenvalues (asc): " + ", ".join(f"{x:.7f}" for x in evals))
    s.append("Soft-mode eigenvector: (" + ", ".join(f"{x:.7f}" for x in v_soft) + ")")
    s.append(f"||chi||_K (computed): {chi_norm_K:.6f}")
    s.append(f"||chi||_K (pinned)  : {keq_norm_pin:.6f}")
    s.append(f"Lambda_chi (calc)  : {Lambda_chi_calc:.6f}")
    s.append(f"Lambda_chi (pins)  : {Lambda_chi_pin:.6f}")
    s.append(f"Lambda diff         : {Lambda_chi_calc - Lambda_chi_pin:.6e}")
    s.append(f"Alignment cos(theta): {cos_theta:.7f}")
    txt = "\n".join(s) + "\n"

    print(txt, end="")
    with open(ROOT / "stdout.txt", "a", encoding="ascii") as f:
        f.write(txt)

if __name__ == "__main__":
    main()
```

keq.json (input) Symmetric positive-definite equilibrium kinetic metric in the $(\ln \alpha_s, \ln \alpha_2, \ln \alpha)$ basis.

```
{
  "K_eq": [
    [1.2509, -0.6202, -0.1813],
    [-0.6202, 1.5128, -0.1633],
    [-0.1813, -0.1633, 3.2362]
  ],
  "notes": "Equilibrium kinetic metric Keq in (ln alpha_s, ln alpha_2, ln alpha)."
}
```

src/ward_flatness_stub.py (optional)

```
#!/usr/bin/env python3
def betaXi_over_logQ(alpha_s, alpha2, alpha_em, betas):
    # beta_Xi = 16*beta_s/alpha_s + 13*beta_2/alpha_2 + 2*beta_em/alpha
    return 16*betas["beta_s"]/alpha_s + 13*betas["beta_2"]/alpha2 +
         2*betas["beta_em"]/alpha_em

def normalized_F_sigma(betaXi, sigma_chi): return betaXi / sigma_chi

if __name__ == "__main__":
    print("Stub: provide (Q, alpha_s, alpha_2, alpha, betas)
    grid and accumulate |F_sigma| stats.")
```

src/snf_check.py (optional; needs sympy)

Exact-integer Smith normal form (SNF) + unimodular transport; certificate that `chi = (16,13,2)` arises from integer right-kernel of `DeltaW_EM`. *Optional; build passes without SymPy.*

```
#!/usr/bin/env python3
# snf_check.py -- exact-integer SNF + primitive kernel for DeltaW_EM (version-robust)

from sympy import Matrix, ilcm, igcd, ZZ

# Define the DeltaW_EM matrix in the (SU3, SU2, EM) basis
A = Matrix([[8, 8, 224],
            [0, 1,  18]])  # DeltaW_EM

U = D = V = None

# 1) Try Matrix method (newer SymPy)
if hasattr(Matrix([[1]]), "smith_normal_form"):
    try:
        U, D, V = A.smith_normal_form()  # U*A*V = D
    except Exception:
        U = D = V = None

# 2) Fallback: module function (older SymPy), normalize return signatures
if D is None:
    try:
        from sympy.matrices.normalforms import smith_normal_form as snf_func
        try:
            out = snf_func(A, domain=ZZ, calc_transform=True)
        except TypeError:
            out = snf_func(A, domain=ZZ)

        # Normalize various return signatures
        if isinstance(out, tuple):
            if len(out) == 3:  # could be (D,U,V) or (U,D,V)
                for Dm, Um, Vm in [(out[0], out[1], out[2]),
                                   (out[1], out[0], out[2]),
                                   (out[2], out[0], out[1])]:
                    try:
                        if Um*A*Vm == Dm:
                            D, U, V = Dm, Um, Vm
                            break
                    except Exception:
                        pass
            elif len(out) == 2 and isinstance(out[1], tuple) and len(out[1]) == 2:
                D, (U, V) = out
        else:
            D = out  # D only
    except Exception:
        pass

# --- Validate SNF if available ---
m, n = A.shape
if D is not None:
    assert D.shape == (m, n)
    # rank = number of nonzero diagonal entries
    r = sum(1 for i in range(min(m, n)) if D[i, i] != 0)
    assert r == 2, f"Expected rank 2; got {r}"
```

```
    # columns beyond rank must be all zeros (here: the 3rd column)
    for j in range(r, n):
        assert all(D[i, j] == 0 for i in range(m)), "Trailing column not zero in D"
else:
    r = 2  # expected for this A; continue without D/U/V assertions

# --- Kernel from SNF if V present (preferred) ---
chiZ_snf = None
if V is not None and D is not None:
    chiZ_snf = V[:, -1]  # last column spans ker_Z(A) since n - r = 1
    if chiZ_snf[-1] < 0:
        chiZ_snf = -chiZ_snf

# --- Fallback: rational nullspace, integerize,  primitive ---
chiQ = A.nullspace()[0]          # rational kernel
den = 1
for q in chiQ:
    den = ilcm(den, getattr(q, 'q', 1))   # LCM of denominators
chiZ_rat = den * chiQ                      # integer entries now
g = abs(int(igcd(*[int(v) for v in chiZ_rat])))
chiZ_rat = chiZ_rat.applyfunc(lambda v: v // g)  # elementwise integer divide
if chiZ_rat[-1] < 0:
    chiZ_rat = -chiZ_rat

# Choose kernel (prefer SNF path if available)
chiZ = chiZ_snf if chiZ_snf is not None else chiZ_rat

# Checks
assert A*chiZ == Matrix([0, 0])
assert tuple(chiZ) == (-10, -18, 1)  # EM-basis primitive kernel

# Unimodular transport to (alpha_s, alpha_2, alpha)
M = Matrix([[-5, -3, -2],
            [ 2,  1,  1],
            [ 2,  1,  0]])
assert M.det() in (1, -1)
chi_gauge = M.T * chiZ
assert tuple(chi_gauge) == (16, 13, 2)

# Report
if D is not None:
    diag_list = [D[i, i] for i in range(min(m, n)) if D[i, i] != 0]
    print("SNF invariant factors (diagonal):", diag_list)  # expected [1, 8]
else:
    print("SNF transform matrices not available in this SymPy build;
    used rational nullspace path.")
print("Primitive kernel in (SU3,SU2,EM):", tuple(chiZ))
print("Transported kernel in (alpha_s, alpha_2, alpha):", tuple(chi_gauge))
print("All checks passed.")
```

build.sh

```
#!/usr/bin/env bash
```

```
set -euo pipefail
mkdir -p src

python3 src/omega_chi.py | tee /dev/stderr
python3 src/gate_null.py | tee -a /dev/stderr

# Optional checks (won't fail the build)
python3 src/ward_flatness_stub.py || true
python3 -c "import sympy" >/dev/null 2>&1 && python3 src/snf_check.py || true

python3 checksums.py
echo "OK"
```

checksums.py

```
#!/usr/bin/env python3
import hashlib, os

def sha256(p):
    h = hashlib.sha256()
    with open(p,'rb') as f:
        for chunk in iter(lambda: f.read(8192), b''):
            h.update(chunk)
    return h.hexdigest()

def main():
    outs = [p for p in ["results.json","stdout.txt"] if os.path.exists(p)]
    with open("SHA256SUMS.txt","w") as f:
        for p in outs:
            s = f"{sha256(p)}  {p}"
            print(s)
            f.write(s+"\n")

if __name__ == "__main__":
    main()
```